UNIVERSITY OF MESSINA

Department of Chemical, Biological, Pharmaceutical and Environmental Sciences

Ph.D. course in Applied Biology and Experimental Medicine

XXXVI Cycle

SSD: BIO/07

Investigation of the response in two demersal fish species: *Coris julis* and *Serranus scriba* under ocean acidification conditions in the CO_2 vent of Ischia (Italy)

Ph.D. Thesis of:

Luca Pagano

Tutor Unime:

Prof. Gioele Capillo

Tutor SZN:

Dr. Pierpaolo Consoli

Coordinator:

Prof. Emanuela Esposito

Academic Year 2022/2023

INDEX

Abstract

In the last 200 years, the CO_2 concentration in the atmosphere has significantly increased because of human activities. About 30% of the anthropogenic CO_2 emissions in the atmosphere have been absorbed by the oceans, causing a decrease in the seawater pH of 0.1 unit. Climate predictions suggest that pH will further decrease by 0.3 units by 2100 reaching the value of 7.3 in 2300.

Ocean acidification caused by anthropogenic activity is known to affect wild animals in the ocean with unforeseen consequences for survival and biodiversity. Evaluating how marine species might adapt to predicted environmental conditions in the near future is challenging. The present study is directed at resident wild fish that inhabit natural acidified seawater due to venting of CO_2 by hydrothermal vents. The direct effects of acidification, as predicted in climate change scenarios, were investigated in the Mediterranean rainbow wrasse *Coris julis* (Linnaeus, 1758) and painted comber *Serranus scriba* (Linnaeus, 1758) by the use of a natural acidified area. The study was conducted in the Ischia shallow vent systems (Gulf of Naples). The environmental conditions around Ischia provide a natural laboratory and a unique opportunity to study the response of the organisms to future climate change conditions. At this aim, a mineralogical and a molecular approach were carried out:

1) structure and composition of fishbone Hydroxyapatite (HAP) was evaluated in these two species in order to highlight potential physiological effects due to exposure to natural acidification.
2) 16S sequencing was carried out to determine the response of fish endogenous microbiota to acidified conditions.

The results obtained from this project suggest that both species respond to environmental conditions, even though in different ways. The skin microbial composition was species-dependent, whereas the mineralogical features of skeleton were mainly influenced by age. However, the skin microbial community

of *S. scriba* exhibited a significant disturbance when it was associated with low pH site compared to *C. julis*, which showed no particular variation between sites, thus indicating that there is a species-specific response to environmental conditions. Moreover, a moderate skeleton maturation was also found in fish exposed to acidified conditions than in control.

In light of the obtained results, there is a need for further clarity regarding the mechanisms that fish engage under unusual environmental conditions, reflecting the future climate change scenario predicted for 2100. The results also confirm that these naturally acidified areas of CO_2 vents represent a valuable resource for researchers who intend to study the responses of marine organisms to acidification.

General introduction

Ocean acidification

Human activities from the beginning of the industrial revolution (1760-1780) have resulted in an increase of CO_2 concentration in the atmosphere (IPCC 2014; Gattuso et al. 2015). In the last two centuries indeed, CO_2 levels in the atmosphere have increased from 280 ppm of the pre-industrial age (Petit et al. 1999; EPICA community members 2004; Siegenthaler et al. 2005) to the modern 420 ppm registered in 2023 in Mauna Loa Observatory-Hawaii (Fig.1).

Carbon dioxide, like other gases has absorbed by the seawater due to the seawater natural sink capacity. Carbon dioxide in the atmosphere is a nonreactive gas but, when dissolved in seawater it takes part in several chemical, physical, biological and geological reactions causing the alteration of the carbonate equilibrium. One of the overall effects of CO_2 dissolving in seawater is to increase the concentration of hydrogen ions ([H+]). This is the result of an initial reaction between water (H_2O) and CO_2 to form carbonic acid (H_2CO_3). This weak acid readily dissociates into bicarbonate (HCO3-) and hydrogen ions (Doney 2009).

$$CO_2(atm) \rightleftarrows CO_2(aq) + H_2O \rightleftarrows H_2CO_3 \; H^+ + HCO_3^- \rightleftarrows 2H^+ + CO_3^{2-}$$

Thus when atmospheric CO_2 dissolved in seawater, the oceans increase in acidity. Nevertheless, seawater alkalinity buffers the effect of the CO_2 reaching the water from the atmosphere maintain its values within relatively narrow limits, between 7.5 and 8.4 (Nybakken, 2004). Thus, the resultant solution is still slightly alkaline. Since the emission rate of anthropogenic CO_2 in the atmosphere is increasing, the capacity of the carbonate buffer to restrict pH changes is diminishing. For this reason, when CO_2 dissolves, the chemical processes that take place reduce some carbonate ions, which are required for the ocean pH buffer (Sabine et al. 2004)

(Skirrow & Whitfield, 1975; Broecker &Takahashi, 1977; Broecker et al., 1979; Caldeira e Wickett 2003; Feely et al. 2004; Orr et al. 2005).

During the last 250 years, over 30% of the anthropogenic CO_2 emissions has been absorbed by the seawater (Sabine et al. 2004) causing the decrease of oceanic pH level that can be quantified as 0.1 unity in the year 2000 and by means of simulation models it is estimated to decrease further by 0.3 unity by the year 2100 (Caldeira e Wickett 2005) to reach pH values of 7.3 by the year 2300 (according to the IPCC scenario).

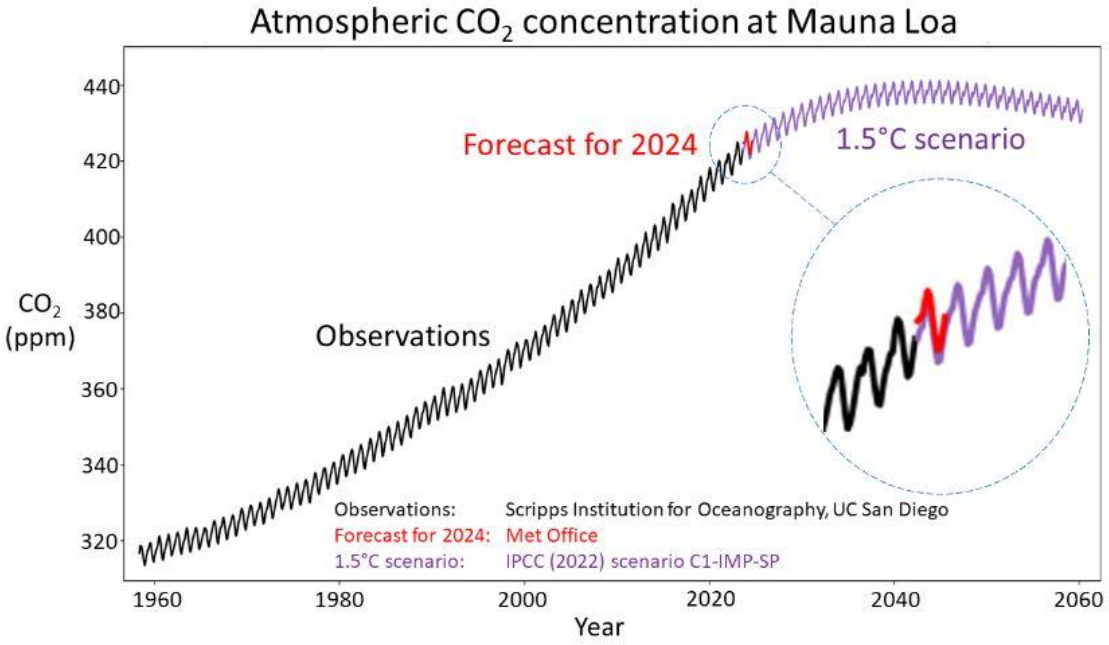

Figure1. Monthly CO_2 concentrations from observations up to 2023 (black) and a future projection consistent with limiting global warming to 1.5°C (purple). Also shown is the Met Office forecast for 2024.

Effect on marine organisms

Ocean acidification is happening so fast that it raises serious concerns about the response of marine organisms that might not be able to adapt to changing environmental conditions on such a short time scale (Guinotte e Fabry 2008).

Moreover, this phenomenon is projected to impact all areas of the ocean, from the deep sea to coastal areas (Orr et al. 2005; Feely, Doney, e Cooley 2009; Feely et al. 2010), with potentially wide-ranging impacts on marine life (Doney 2009). Several studies, aimed at understanding how the projected changes in carbonate chemistry will affect marine species, communities, and ecosystems were performed on laboratory and mesocosm experiments. In this regard, there is a significant variance in biological responses between taxonomic groups to ocean acidification that has a significant negative effect on survival, calcification, growth, development and abundance (Kroeker et al. 2013).

In particular, marine organisms that build hard structures made of calcium carbonate minerals including calcified algae, corals, mollusks, and the larval stages of echinoderms are generally considered to be more negatively affected by the acidification (Kroeker et al. 2010; 2013). Although all calcareous organisms show a reduction in growth of a similar magnitude and a reduction in calcification was observed in mainly in corals and coccolithophores, molluscs are one of the groups most sensitive to acidification where a significant reduction in calcification, growth, development (and survival when the exposure regards the early life stages) is observed. Another taxonomic group affected by acidification are calcified algae, for which photosynthesis is reduced. This sensitivity in calcified algae is also apparent in experiments that tested for impacts on abundance, where calcified algae have a much greater mean reduction (80%) in percent cover/abundance in acidified conditions than other groups. In addition, corals suffer significant mean reductions in abundance (47%) in acidified treatments.

More active organisms, such as mobile crustaceans and fish, may be less sensitive to acidification due to their ability to cope with extra-cellular acidosis thanks to their acid-base regulation (Melzner et al. 2009) whereas some fleshy algae and diatoms may benefit, although marginally, from the same conditions (Koch et al.

2013). Nevertheless, the chemical imbalance in seawater was found to influence physiology (growth rate development, survival and reproduction) and behaviour of various species of fish (Philip L Munday et al. 2008; Heuer e Grosell 2014; Cattano et al. 2018; Mirasole et al. 2021) but many other aspects are still unknown. Because of their ability to regulate their acid-base, fish have been considered to be able to tolerate extra-cellular acidosis (Melzner et al. 2009). The olfactory, visual and auditory functions (Dixson, Munday, e Jones 2010; Philip L. Munday et al. 2009; Simpson et al. 2011), reproduction (G. M. Miller et al. 2013), calcareous structure (Bignami et al. 2013; Mirasole et al. 2021; Leung et al. 2022) behavior and neurosensory functions (Domenici et al. 2012; Philip L. Munday et al. 2014; Nilsson et al. 2012), habitat alteration and interaction with other species (McCormick, Watson, e Munday 2013; Nagelkerken e Connell 2015) however, have all been tested under acidifying conditions, both direct and indirect effects. Different life stages will be affected differently by climate change, with larvae and juveniles being more susceptible (Baumann, Talmage, e Gobler 2012; Ishimatsu et al. 2004; Pankhurst e Munday 2011). For example, larvae exposed to acidified seawater (approximately 1000 ppm of CO_2 - pH = 7.8) lost their capacity to distinguish between predatory and non-predatory species' chemical signals (Dixson, Munday, e Jones 2010). Some temperate fish species living in Volcanic CO_2 seeps showed an increase in population size in the presence of elevated CO_2 due to increased gene expression in gonad tissue (Petit-Marty et al. 2021a). Moreover, the effects of ocean acidification can also be determine changes in skin microbial composition have been described after acute short-term acid stress in *Colossoma macropomum* in laboratory conditions (Sylvain et al. 2016).

However, studies suggest a species-specific response, with various sensibility at different CO2 levels. For instance, (P. Munday et al. 2011a) observed no effects on spiny damselfish otolith calcification at high CO_2 levels (850 μatm), while (P. L. Munday et al. 2011b) and (Checkley et al. 2009) highlighted otolith

hypercalcification in white sea bass larvae exposed to 993 and 2558 μatm. To date, most information available on fish response to ocean acidification have been obtained in closed systems, and only a few studies have been carried out *in situ* (Cattano, Giomi, e Milazzo 2016; Nagelkerken e Connell 2015; Petit-Marty et al. 2021b; Philip L. Munday et al. 2014).

Hydrothermal vents

Knowledge on organism responses to pH decrease were obtained almost completely by lab experiment. However, there are some localised areas on the oceans were for different reasons (estuaries, upwelling areas, volcanic CO_2 vents) a decrease of pH occurs. Among the others, Hydrothermal vents represent a resource for scientist which feature of the conditions to formulate hypotheses of climate change future scenarios on marine ecosystem.

Conventionally hydrothermal vents may be diversified into shallow and deep according the depth. Thus, the vents found up to 212 m deep are considered Shallow, while those located beyond 212 m depth are considered deep (Tarasov et al. 2005). Although a first distinction can be made according to the depth at which they occur, a high degree of variability between different vents is due to temperature differences and the presence/absence of certain compounds and metals, making them completely different environments. In shallow hydrothermal vents, the temperature of the venting fluids ranges between 10 and 119 °C (Dando, Hughes, e Thiermann 1995; Tarasov et al. 2002), while in deep system the temperature of venting fluids can exceed 400 °C, sea water penetrates deep inside the crust and the vent fluids are formed at up to 1200 °C (Barriga, F.F.A 1997). As regards the chemical aspect, differences in concentration of elements between hydrothermal areas are very pronounced (Krasnov and Sudarikov, 1990; Gavrilenko, 1997; Sedwick and Stuben, 1996). Such high difference is

determinated by the fluids' composition. In general, deep hydrothermal vents fluids are characterized by high concentration of reduced substances and metals, and extremely high values of H_2, H_2S, and H_4 (Tarasov et al. 2005). A pronounced feature of shallow-water vents is the presence of a gas phase (absent in the deep-sea) and much greater enrichment in O_2 compared to deep-water vents (Tarasov et al. 2005).

Marine CO_2 vents are abundant in the Mediterranean, especially around Italy and Greece on arc volcanoes, back-arc basins, and hot spot volcanoes. The Mediterranean hydrothermal complexes are characterized by a range of 0–1200 m depth, with temperatures ranging between 13–135 °C. All the Mediterranean sites share the presence of a well-noted gaseous composition (CO_2, H_2S, CH_4). Not all Mediterranean vents are characterized by hot emissions, as revealed by the low temperature value (between 13–25 °C) detected in the deep Ischia Island (Fig. 2), Palinuro Cape, some areas of the Panarea Volcanic Complex, Yali, Methana, Nisiros, Santorini, and Kos HVs.

Although these are circumscribed areas in which pH variations cannot be controlled, the use of natural CO_2 vents as 'natural laboratories' on the other hand provides variables that cannot be reproduced in the laboratory and mesocosm.

On wild experiments indeed, allow to investigate on long term effects to exposure to high pCO_2/low pH values on natural populations which continue to maintain interactions with the surrounding environment (currents, nutrients and species interactions) (Barry et al. 2010).

Figure 2. The underwater volcanic vents occur in a semi-submerged cave at 5 m depth, release continuously gaseous emissions (92%–95% CO_2, no sulfur), and do not elevate temperature. Copyright: https://communities.springernature.com/

Study area

The experiments were conducted at CO_2 vent system of the Island of Ischia. Marine CO_2 vents are abundant in the Mediterranean Sea and the Island of Ischia (Tyrrhenian Sea, Italy) is already widely utilized to assess the effects of OA on flora and fauna communities (Hall-Spencer et al. 2008; Kroeker et al. 2011; Mecca et al. 2020; Signorini et al. 2023) (Tyrrhenian Sea, Italy). Shallow and cold vent occur at 0.5 – 3m depth on both sides of the Castello Aragonese adjacent to a steeply sloping rocky shore causing a decrease of the seawater pH in some area also down to 6.50 (Hall-Spencer et al. 2008; Kroeker et al. 2011). The emitted gas is almost entirely composed by CO_2 (90–95%) with no toxic sulphur compounds

(Hall-Spencer et al. 2008; Foo, Byrne, e Gambi, 2018; Gambi et al. 2010). Although the presence of natural CO_2 vents affects the abundance of most species, it seems not to cause a disturbance for several fish species that are widely distributed on both sides of the Castello Aragonese.

The use of high site fidelity species (March et al. 2010; Goverts, Nührenberg, e Jordan 2021) represents a useful tool to directly address the likely impact on fish physiology and health of changing CO_2 of fish naturally exposed to high pCO_2/low pH conditions.

The sampling sites included one acidified site on the north side of the Castello Aragonese (40°43’55” N, 13°57’51” E) and one ambient pH site located 2 Km far away from the vents, in front of S. Pietro beach (40°44'48"N 13°56'40"E) used as control station. The vents area on the north site of the Castello Aragonese is characterized by the strong bubbling activity of gas composed almost completely of CO_2 (90.1 - 95.3%) with no toxic sulphur compounds and with no variation on temperature and salinity if compared to the surrounding waters (Hall-Spencer et al. 2008; Foo, Byrne, e Gambi, 2018; Gambi et al. 2010). The CO_2 emissions cover an area of 5000 m2 and host a high diversity level of teleost leading a recorded average pH of 7.21 ± 0.34 (Kroeker et al. 2011; Ricevuto et al. 2014; Foo, Byrne, e Gambi, 2018) in the studio area comparable with values predicted for the year 2300 (Caldeira e Wickett 2005). The site off S. Pietro beach almost 2 km northwest from Castello Aragonese, was chosen as control given the presence of similar conditions and environmental features (exposure, depth, habitat complexity, species richness) and the lack of volcanic activities and pH values of 8.1.

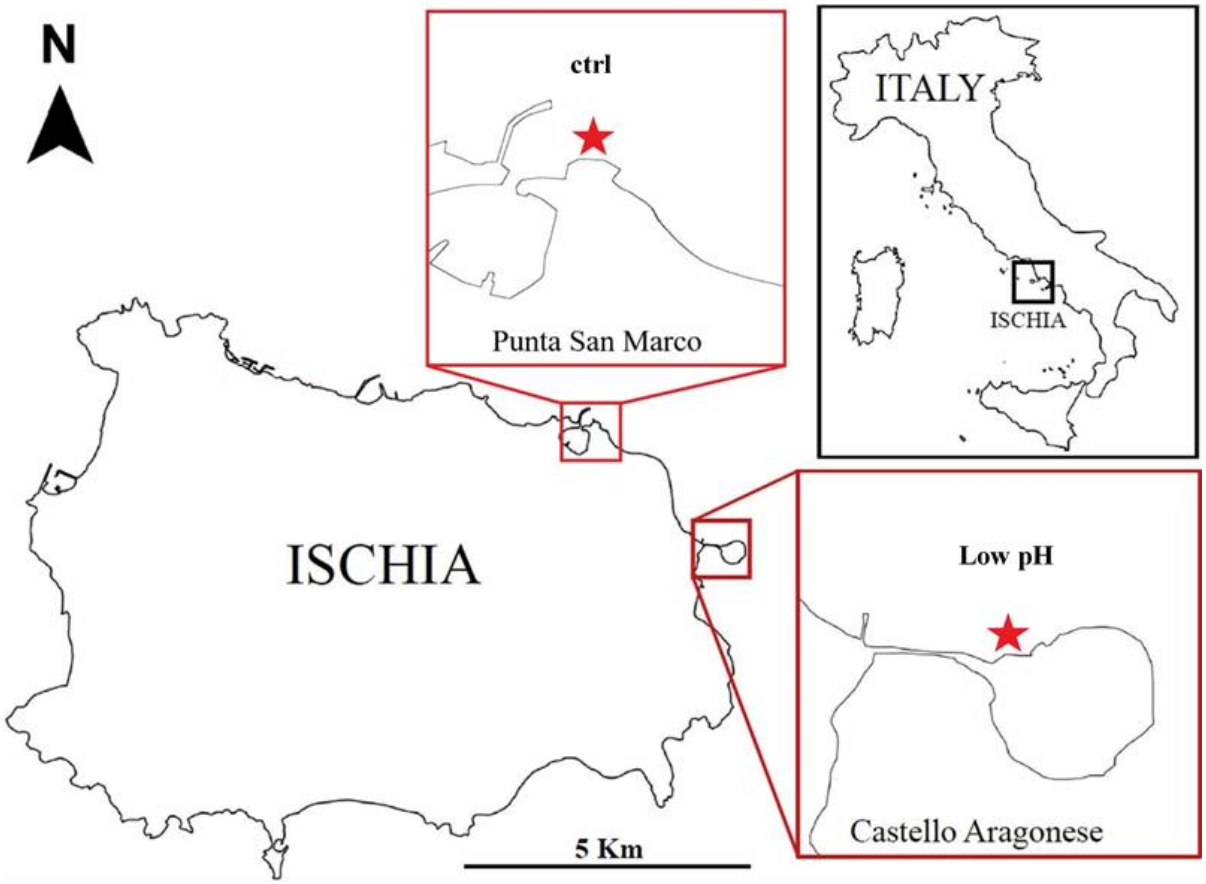

Figure 3. Map indicating the location of the study area in Ischia Island (Italy).

Aim and goals

The aim of this PhD project was to evaluate the responses of two marine teleost species exposed to pH reduction, as potential predictive scenario of climate change for 2100. Fish are a key biological component whose monitoring is relevant not only from the ecological standpoint, but also for the economic repercussions (*i.e.* impacts on seafood - Branch et al. 2013). Hence, the present study was focused on samples collected from natural acidified seawater due to venting of CO_2 by hydrothermal vents, in the area of Castello Aragonese (Ischia). The species selected are the Mediterranean rainbow wrasse *C. julis* and the painted comber *S. scriba*. These two species are small, territorial marine fish inhabiting rocky and seagrass meadows areas (Costello et al, 1991) of the shallow

water of the whole Mediterranean Sea and in eastern Atlantic (Fischer *et al.* 1987; Bauchot,1987).

The Mediterranean rainbow wrasse, (*C. julis*) is a demersal labrid species, and is the only specie of its genus and it can be found in the Mediterranean, usually from a few metres to 50 m depth (Quignard and Pras 1986). It is a protogynous hermaphroditic species, where part of the females of a population turn into males.

The painted comber, *S. scriba* (Linnaeus, 1758) is a demersal serranid species generally found along the continental shelf covered with *Posidonia oceanica* or *Cymodocea* spp. beds at 0.5–150 m depth. It is a simultaneous hermaphrodite (Fischer and Petersen, 1987).

The choice of two different teleost species provides the chance to assess species-specific characteristics but also more global responses to acidification. Using samples collected from the natural environment means the results are likely to be more representative of the fluctuating environmental conditions. Ocean acidification caused by anthropogenic activity is known to influence physiological processes causing reduced growth of calcified structures, otolith development, and fertilization success. The investigation on skeleton mineralization process might allow us to evaluate any possible premature skeleton ageing as a response to the effect of OA on CO_2 vent.

Furthermore, environmental stress as acidification might modulate resident microbiota on the mucosal surfaces (epithelia) on skin, gut and gills (Butt e Volkoff 2019). The global characterization of fish microbiota can provide information about the relative abundance of potentially pathogenic and non-pathogenic bacteria and their interaction with the host, contributing to the development of measures for the prevention and control of disease.

In the light of above mentioned, the goals of the PhD project were:

1) to obtain information that could enhance our understanding of how the skin and gills microbial communities respond under lower than normal pH conditions.
2) assess the elemental composition and the mineral features of the skeleton of fish naturally exposed to high pCO_2/low pH conditions against fish living in two normal pH conditions (controls).

A molecular and a mineralogical approach were carried out to assess how natural exposure of fish to acidified conditions shifts in skin microbiome and skeleton development.

1. LONG-TERM EFFECTS OF HIGH CO_2 LEVEL EXPOSURE ON FISH MICROBIAL COMMUNITY

1.1 Introduction

Teleost fish's first defence against biological, physical and chemical hazards are the mucosal surfaces (epithelia) on skin, gut and gills and olfactory organs (Salinas 2015; Lazado e Caipang 2014). All four mucosal organs contain mucosa-associated lymphoid tissues (MALT) which are involved in the detection, recognition and defence against pathogens (Salinas 2015). These four MALTs are called gut-associated lymphoid tissue (GALT), gill-associated lymphoid tissue (GIALT), skin-associated lymphoid tissue (SALT), and nasal-associated lymphoid tissue (NALT). Thus, teleost MALT is a primary immune response site with strong activity from the innate immune system and antimicrobial peptides (Ángeles Esteban e Cerezuela 2015). All mucosal surfaces are unique microenvironments for non-pathogenic and co-habitant microorganisms and they likewise provide another layer of defence by antagonising pathogens through the production of bacteriocins, H_2O_2, and antimicrobial peptides and other inhibitory compounds. The diverse array of microorganisms found in association with fish tissues such as stomach, gills, skin, and even internal organs is known as fish microbiota. These microbes may include viruses, fungus, bacteria, or archaea. Nevertheless, fish like other organisms (e.g., human) could hosts also pathogenic bacteria. The host-microbe interactions are ubiquitous and play important roles in the host's biological activities, such as nutritional acquisition and immunology, as well as competing pathogen suppression. In turn, the host supports the nutrition pool and colonisation of internal and external microbes. When an imbalance (dysbiosis) occurs, it can shift the microbiota composition towards pathogenic species and facilitate disease outbreaks (Brugman et al. 2018; Wynne et al. 2020).

The microbial community associated to fish tissues might easily be modulated by the environmental conditions (Butt e Volkoff 2019). Teleost fish provide an excellent repertory of host species for studying the nature of vertebrate microbial communities (Nayak 2010) and the mechanisms influencing animal-associated microbiomes (Lescak e Milligan-Myhre 2017). Among the environmental variants, the rising levels of carbon dioxide may have a greater influence on the microbiome of aquatic hosts.

The skin microbiome is in continuous contact with the environment. Among the others, the microbial community of the skin is greatly influenced by environmental perturbations that impair host fitness(Byrd, Belkaid & Segre, 2018; Kuziel e Rakoff-Nahoum 2022). Skin mucus is an important component of fish immune systems and contains various immunoglobulins, mucins, antimicrobial peptides, and other mucosal biomolecules that protect the fish from pathogens (Tiralongo et al. 2020).

Changes in skin microbial composition have been described after acute short-term acid stress in tambaqui (*Colossoma macropomum*), a freshwater fish found in the Amazon river (Sylvain et al. 2016).

1.2 Materials and Methods

1.2.1 Fish samples collection and processing

S. scriba and *C. julis* individuals were collected in July 2023 from two different locations along Ischia Island. Fish were sampled in both sites between 2 and 4 m depth in snorkelling with baited hook, placed in sterile bags and transported to the lab. The 40 specimens sampled were measured to the nearest 0.1 cm to obtain the total length (TL) and weighed to the nearest 1 g for total mass (TW) and immediately dissected, and tissue collected and placed in RNA later for preservation. From each fish the following tissues were collected:

1) about 1 cm x 1 cm of skin was collected removing as much muscle as possible;
2) about 20 scales;
3) 1 -2 gill bars plus filaments;
4) about 1 cm long piece of gut taken immediately after the stomach.

The samples were preserved with RNAlater avoiding dilution with water and respecting a ratio 1/10 between sample and RNA later to ensure an optimal preservation. The samples in RNAlater were stored at 4°C overnight (to allow the solution to thoroughly penetrate the tissue), then the tubes containing the samples were moved to – 20°C until the extractions carried out at CCMAR (Faro, Portugal).

Genomic DNA was extracted in order to sequence 16S rRNA and determine how the microbiome of the gills and skin are affected by environmental conditions. Extracted genomic DNA quality was determined and then used for nanopore sequencing. Bioinformatics analysis and statistical analysis were carried out. 40 individuals were sampled for molecular analysis, 20 specimens of each species:

10 from the low pH site and 10 from the control site. All 40 samples were used for DNA extractions.

1.2.2 DNA extraction

DNA was extracted from fish skin, using a DNAse Blood & Tissue Kit (Qiagen, Germany) with some modifications.

About 30 mg of skin, gills and gut and ~ 15 mg of scales stored in RNA later were collected in tubes with 400 µl of lysis mix (200 µl of lysis buffer 20 mM Tris-HCl, pH 8, 2 mM sodium EDTA; 1.2 % Triton X-100; 40 mg/ml lysozyme mixed with 200 µl of AL buffer provided by the Qiagen kit). Afterward, approx. 400 mg of 0.1 mm zirconia/silica beads (Biospec) were added. The tubes were maintained on ice until mechanical disruption, which was carried out at room temperature in a Tissue Lyser (Qiagen, Germany) for 3 cycles of 5 min at 25 Hz.

After the mechanical disruption of samples in the lysis mix the samples were incubated for 30 min at 37°C with the lysozyme (80 µl of 100 mg/ml lysozyme solution per sample, included in the lysis mix), followed by 30 min at 56°C with proteinase K (25 µl of 20 mg/ml). Tubes were centrifuged for 1 min at 4300 ×*g* to pellet the beads, and the lysate was collected into a clean microcentrifuge tube and treated with RNase (10 µl of 10 mg/ml solution) for 10 min at room temperature, and then 0.5 volumes of 100 % ethanol were added. The lysate mix was then purified using the column supplied in the DNeasy Blood & Tissue kit. DNA was eluted into two tubes in 40 µl of Tris- HCl (10 mM, pH 8). DNA quality and integrity were analysed using a Nanodrop spectrophotometer and verified on 1 % agarose gel electrophoresis.

Initially a pre-test was carried out on two samples of each type of tissue. The tissues with low quality and integrity were discarded and not used for the study.

Thus, 24 samples in total were selected between skin and gills of both species. For both *C. julis* and *S. scriba*, 3 replicates of skin from both sites were sequenced.

1.2.3 16S rRNA gene microbiome library preparation and sequencing

Each sequencing library was constructed using DNA from individual samples of skin. Library preparation followed the 16S rRNA gene Sequencing Library Preparation protocol for the Illumina MiSeq system, using optimized primers targeting the hypervariable V3 and V4 regions of the 16S rRNA gene (Klindworth et al. 2013). Libraries were paired-ended sequenced (300 bp ×2) on an Illumina Novaseq platform at BKMGENE (previously Lifesequencing S.L.; Münster, German).

1.2.4 Sequence processing and bioinformatics

Raw reads were processed for quality control. They were primarily filtered by Trimmomatic (Bolger, Lohse, e Usadel 2014) (version 0.33) with a window size setted as 50 bp. The low-quality reads were identified and removed by Cutadapt (Martin, 2011) (version 1.9.1) with a maximum mismatch accepted of 20% and minimum coverage of 80%. Paired-end reads obtained from previous steps were assembled by USEARCH (Edgar 2013) (version 10) with a minimum length of overlap of 10 bp, a minimum similarity within the overlapping region of 90% and a maximum mismatch accepted of 5 bp. Chimeras were removad using UCHIME (Fig.4) (Edgar et al. 2011) (version 8.1).

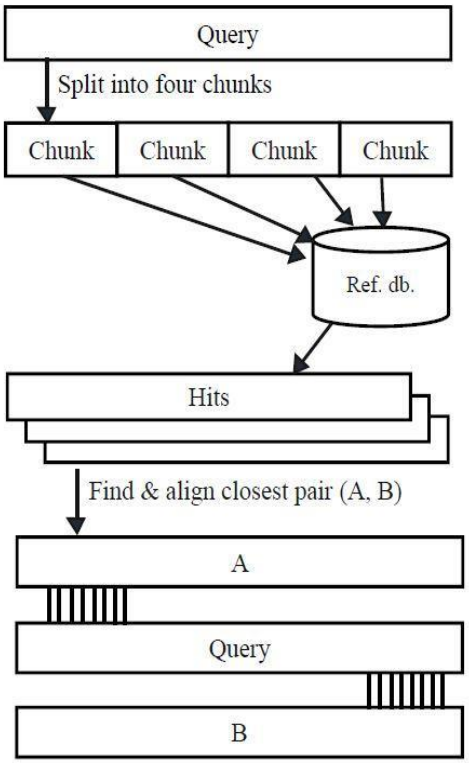

Figure 4. Schematic flow of UCHIME was shown in the following figure. Each query sequence is split into non-overlapped chunks. These chunks were compared with the reference database to identify the best hit of each chunk in the database and further define the two best parent sequences. The query sequence was subsequently compared with the two parent sequences. If a fragment with over 80% similarity to the query sequence is found on both parents, this query sequence will be defined as chimera sequence.

Raw subreads were adjusted to generate Circular Consensus Sequencing (CCS) reads by SMRT Link (version 8.0). Then lima (v1.7.0) was used to identify CCS sequences of different samples by barcode sequence and remove chimeras to obtain high-quality CCS sequences. The sequences were used for classification of operational taxonomic units (OTU) by USEARCH (version 10.0). The sequences were clustered with similarity over 97% (default). Starting from de-noise sequences, ASVs were generated through the DADA2 method (Callahan et al. 2016) in QIIME2 (Bolyen et al. 2018).

Microbial community composition at phylum, class, order, family, genus and species level was revealed by blustering the feature sequences against the

reference database by classify-consensus-blast in QIIME2. Those that did not match the reference database were further classified by classify-sklearn in QIIME. Regarding Alpha Diversity analysis, Chao1 richness estimator and Ace richness estimator were used to measure community abundance. Community diversity was instead measured through Shannon-Wiener's diversity index, Simpson's diversity index and phylogenetic diversity. The rarefaction curve was used to assess whether the amount of sequencing is sufficient to cover all groups.

Functional information were obtained by linking genes in the genome with a network of interacting molecules in the cell by means of KEGG.

1.2.5 Statistical analysis

To analyze changes in species composition on temporal and spatial scales, Beta Diversity Analysis was used. The algorithms of binary Jaccard, Bray-Curtis, weighted Unifrac (bacteria only), and unweighted Unifrac (bacteria only) were used to calculate the distance between samples. Samples were rearranged using principal component analysis (PCA), principal co-ordinate analysis (PCoA), and Nonmetric multidimensional scaling (NMDS) in the R software. After standardized processing (logarithm) according to OUT data, the top 80 species with the largest number are selected and mapped based on the R heatmap. To test whether the differences between groups (two or more groups) are significantly greater than the differences within groups, and thus whether the grouping is meaningful it was used the ANOSIM analysis. Permutational analysis of variance (PERMANOVA) using the adonis function was used to test whether the overall microbial community differed with each variable under analysis. LefSe analysis was performed only on the groups, the number of groups was ≥ 2, and the number of samples contained in each group was ≥ 2. Metastats software (White, Nagarajan, e Pop 2009) was used to conduct the T-test on species richness data

between groups at the taxonomic level of phylum, class, order, family, genus and species for intergroup significance analysis, with a default value of $p \geq 0.05$.

At the correlation level of environmental factors, the correlation analysis of taxonomic diversity, environmental factors, and Alpha index was conducted to obtain the correlation characteristics of taxonomy and environmental factors. Based on the correlation between environmental factors and taxonomy (default genus level) and Alpha index (default Pearson), Mantel analyzed and plotted heatmap and network combinatorial diagram. Based on environmental factors and taxonomy (default parameter, genus level, Pearson correlation, correlation threshold 0.3, correlation p value threshold 0.05, node number 80, edge number 100), correlation network diagram is made.

1.3 Results

1.3.1 Sequencing statistics

A total of 1.721.534 raw read sequences were generated from the 12 samples. Upon that, 1.660.607 clean reads were obtained after PE reads quality control and assembly. Minimum of 76.784 and average of 138.384 clean reads were generated for each sample. The detailed sequencing statistics for each sample is provided in Table 1.

The rarefaction curves indicated saturation or close to saturation coverage for diversity in each sample (Fig.5). Based on the number of detected OTUs, the rarefaction curves also revealed different bacteria richness (between different species and site). In general, *S. sciba* had higher richness values (2846–3367 OTUs), with the highest number of OTUs detected in samples from the control site (Tab. 2) as showed also by the Shannon index (Fig 10a).

Table 1. Details from post-run analysis obtained for each sample.

Sample ID	Raw Reads	Clean Reads	Denoised Reads	Merged Reads	Non-chimeric Reads
C. julis 62 low pH	80.346	76.784	76.708	73.917	71.064
C. julis 64 low pH	140.296	134.020	133.830	127.173	120.823
C. julis 67 low pH	134.235	129.418	128.886	123.794	112.572
C. julis 75 Ctrl	159.984	154.354	153.915	147.649	136.520
C. julis 78 Ctrl	139.865	133.573	133.370	128.327	122.378
C. julis 79 Ctrl	133.128	127.430	127.305	122.788	116.552
S. scriba 50 low pH	160.007	155.024	154.025	143.546	125.259
S. scriba 54 low pH	160.024	155.331	154.412	144.347	124.843
S. scriba 55 low pH	160.148	155.227	154.288	144.798	126.191
S. scriba 60 Ctrl	147.049	142.242	141.275	131.311	108.898
S. scriba 62 Ctrl	151.893	147.397	146.181	134.641	114.466
S. scriba 57 Ctrl	154.559	149.807	148.600	135.541	112.602

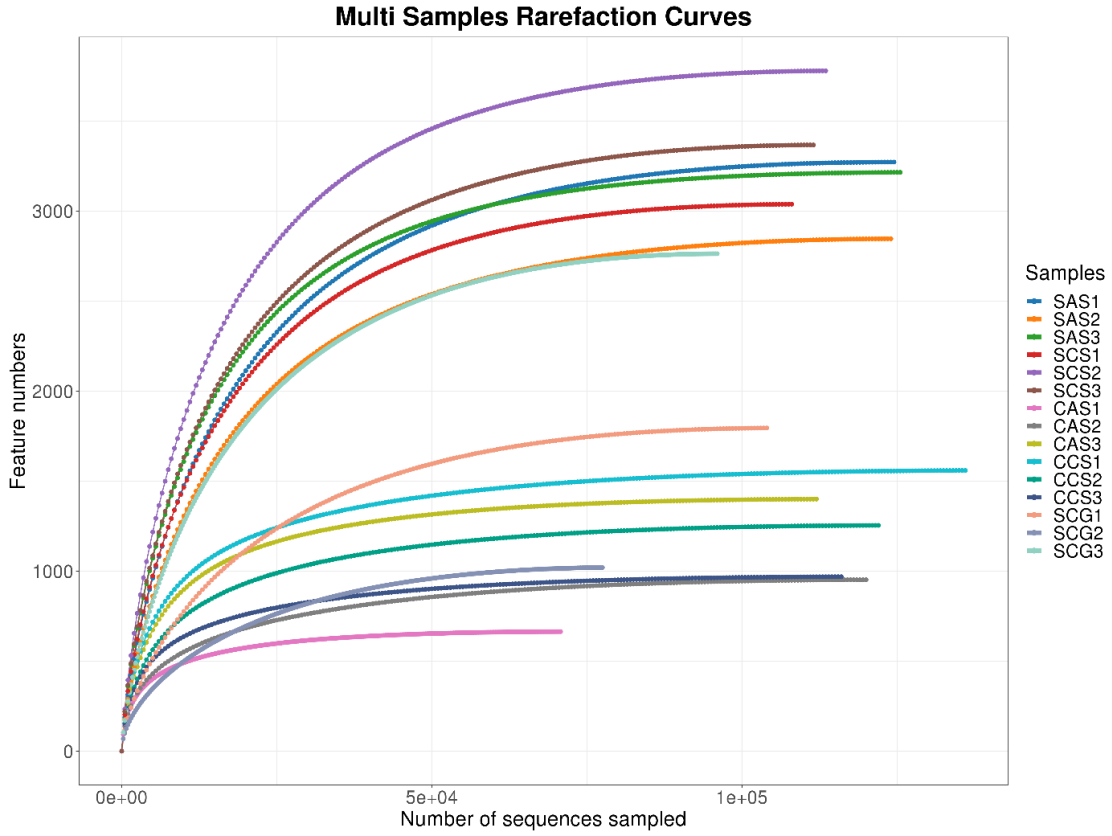

Figure 5. Flat rarefaction curve that sequencing substantially covered all the species in the sample.

Table 2. Diversity indices and OTUs number obtained from fish samples

Sample	OTU_Num	Seqs_Num
C. julis 62 low pH	664	70.909
C. julis 64 low pH	952	120.445
C. julis 67 low pH	1.400	112.269
C. julis 75 Ctrl	1.559	136.205
C. julis 78 Ctrl	1.254	122.069
C. julis 79 Ctrl	969	116.314
S. scriba50 low pH	3.272	124.581
S. scriba54 low pH	2.846	124.175
S. scriba55 low pH	3.215	125.747
S. scriba60 Ctrl	3.038	108.260
S. scriba62 Ctrl	3.779	113.724
S. scriba57 Ctrl	3.367	111.856

1.3.2 Bacterial community composition

The bacterial communities associated with skin of the two fish species showed differences in the taxonomic structure. In the following section the relative abundance of each taxa will be detailed at phylum, family and genus level, expressed as average value between the three replicates for fish species.

The most abundant phyla in the *S. scriba* skin microbial communities were *Proteobacteria* (average relative abundance 34.6% in the total microbial community), with a range between 28.4% and 42% in the samples from the acidified site and between 26.6% to 39.6% in the samples from the control site; followed by *Firmicutes* (average relative abundance 29.8% in the total microbial community), with a range between 27.3% to 35.0% in the samples from the acidified site and between 27.0% to 32.5% in the samples from the control site. The third abundant phylum was represented by *Bacteroidota* (average relative abundance 12.9% of the total microbial community) with higher values in the

samples from the control site (12.6-15.6%) than in samples from the acidified site (9.9-14.4%).

The presence of the group *Thermotogota* was also evidenced (average relative abundance of 10.1% of the total microbial community), with a range between 8.5% to 10.9% in the samples from the acidified site and between 10.0% to 11.8% in the samples from the control site (Fig. 6). *Acidobacteriota* and *Actinobacteriota* were detected in all samples with lower relative abundance (<2.6%).

At family level, the most abundant families were represented by *Vibrionaceae* (average relative abundance of 25% of the total microbial community), with a range comprised between 17.4% and 34.0% in the acidified site and from 16.9% to 30.7% in the samples from the control site; *Petrotogaceae* (average relative abundance of 10.13 % on the total bacterial community) with relative abundance values of 8.5-11% in the samples from the acidified site and 10-11.8% in the samples from the control site; *Lactobacillaceae* (average relative abundance of 5.2 %) in the range 4.3-5.6% and 4.7-6.9% in the samples from the acidified and control sites, respectively. Other groups were represented by: *Lachnospiraceae* (average abundance 3,4 %, range = 2.7-4.1 and 3.2-4.6% in the samples from the acidified and control sites, respectively); *Muribaculaceae* (average abundance 3.5 %, range = 2.7-3.7 and 3.2-4.7% in the samples from the acidified and control sites, respectively); *Enterococcaceae* (average abundance 3.2 %, range = 2.5-3.9 and 3.1-3.3% in the samples from the acidified and control sites, respectively); *Clostridiaceae* (average abundance 2,8 %, range = 3.1-4.5 and 1.5-2.6% in the samples from the acidified and control sites, respectively) (Fig. 7).

In general, in the microbial communities associated with *C. julis* skin a higher percentage of *Bacteroiodota* was detected (average relative abundance of 33% on the total microbial community), ranging between 21.9% and 42.2% in the samples from acidified site, and between 22.1% to 40.6% in the samples from the control site. The second most abundant phylum was represented by *Firmicutes* (average

relative abundance of 19.4% of the total microbial community), ranging between 13.2% and 26.5% in the samples from the acidified site, and between 14.3% to 31.0% in the samples from the control site. The group of *Proteobacteria* was detected less represented in *C. julis* skin. The presence of *Fusobacteriota* member was detected in relative abundance ranging between 5.5% and 16.6% in the samples from the control site (Fig. 6).

Paludibacteraceae was the most abudant family (average relative abundance of 9.12 % of the total microbial community), with a range comprised between 5.9% and 12.6% in the acidified site and from 4.3% to 13% in the samples from the control site; followed by *Weeksellaceae* (average relative abundance of 8.8 % on the total bacterial community) with relative abundance values of 4.5-11.5% in the samples from the acidified site and 5.8-11.4% in the samples from the control site; *Bacteroidaceae* (average relative abundance of 8.2 %) in the range 4.9-11.1% and 4.9-6.2% in the samples from the acidified and control sites, respectively; *Lactobacillaceae* (average relative abundance of 6.19 % on the total bacterial community) with relative abundance values of 1.4-12.6% in the samples from the acidified site and 2.3-13.3% in the samples from the control site. Other groups were represented by: *Fusobacteriaceae* (average abundance 5.44 %, range = 0.7-6 and 2.6-16.6% in the samples from the acidified and control sites, respectively); *Vibrionaceae* (average abundance 4.14 %, range =0-34.15.4 and 0-6.8% in the samples from the acidified and control sites, respectively); *Morganellaceae* (average abundance 2 %, range = 1-3.3 and 0.7-2.5% in the samples from the acidified and control sites, respectively); *Rikenellaceae* (average abundance 2 %, range = 1.9-2.2% in the samples from both the acidified and control sites, respectively) (Fig. 7).

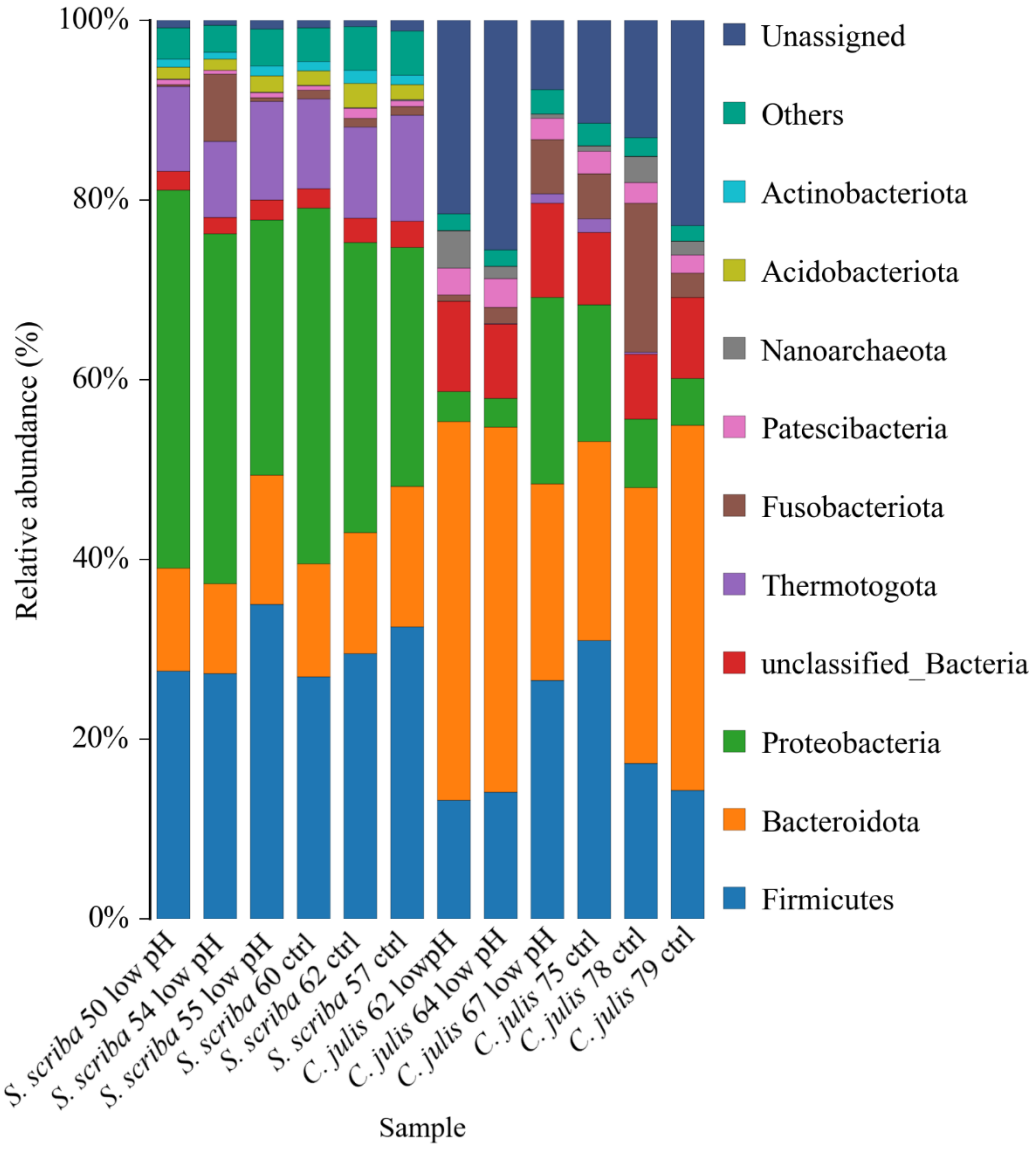

Figure 6. Taxonomic composition of fish skin associated bacterial communities at Phylum level.

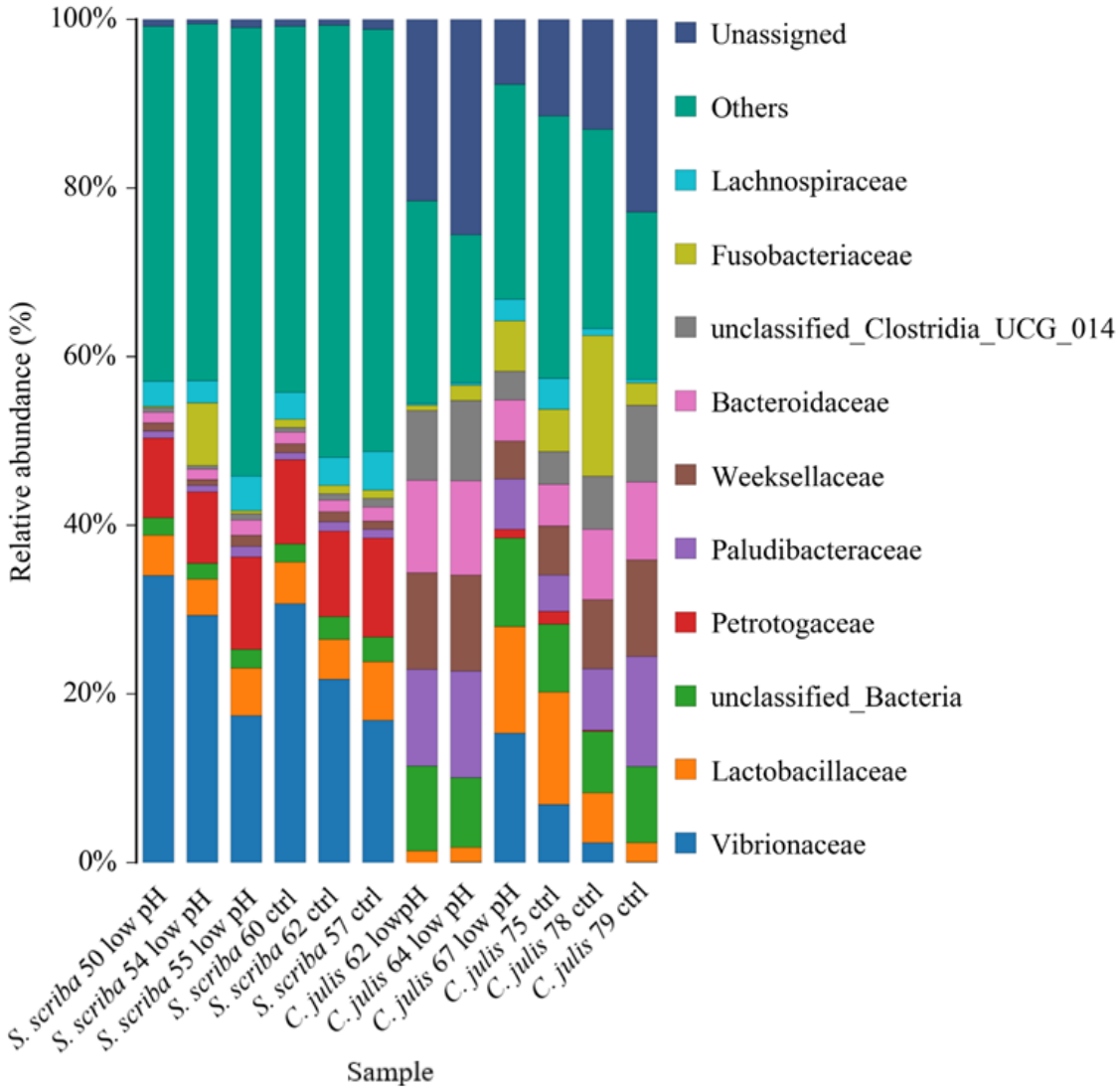

Figure 7. Taxonomic composition of fish skin associated bacterial communities at family level.

The size of the microbiome and common/core bacteria genera were analysed by counting the number of bacterial genera across all samples. In general, the samples of *S. scriba* from both acidified and control sites had the highest number of bacteria genera while *C. julis* had the lowest number which is further low in the acidified site (Fig. 8).

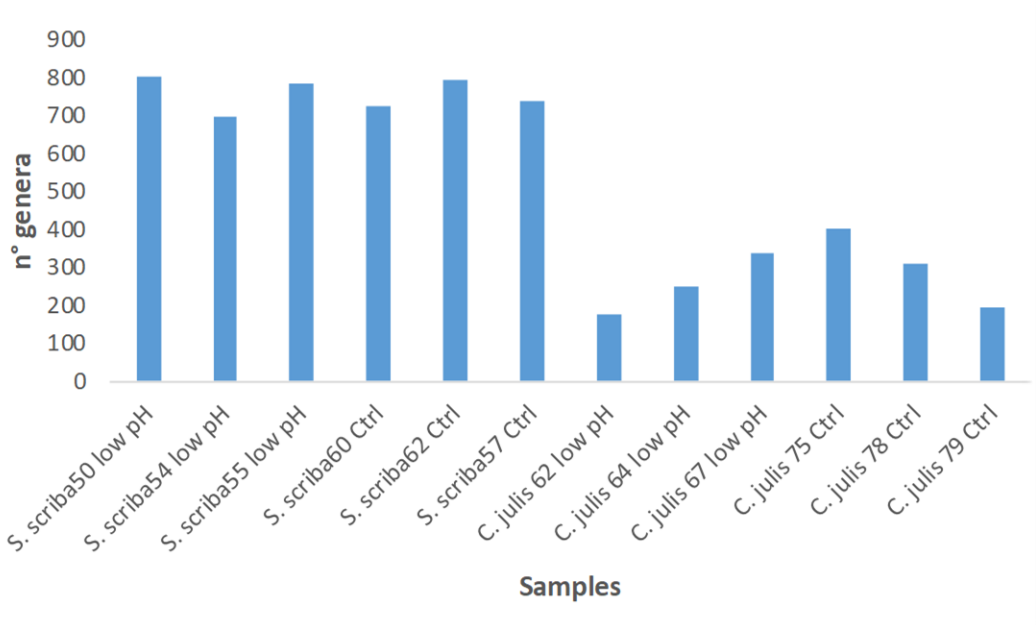

Figure 8. Number of microbial genera in fish skin microbial communities

The microbiota abundance was determined up to the species level, but for higher confidence in OTU assignment, it is only discussed up to the genus level. The bacterial genera detected with an average abundance (between samples) higher than 1 % are listed in Table 3. The clustered heatmaps of relative abundance only include the genera/OTUs with relative abundance >8%. A graphical summary of the five most abundant genera per sample type is presented in Fig. 9. *Photobacterium* was the most abundant genus in *S. scriba* (average relative abundance 16.7 %, comprised between 13.3 and 29.3 in specimens from acidified site and 8.1 and 14.9 in specimens from the control site); followed by *Defluviitoga* (average relative abundance 10.1 %, comprised between 8.5 and 11 in specimens from acidified site and 10 and 11.7 in specimens from the control site) and *Vibrio* (average relative abundance 8 %, comprised between 3.2 and 4.5 in specimens from acidified site and 7.8 and 15.6 in specimens from the control site) . In the species *C. julis* the most represented genus were *Paludibactearaceae* family (average relative abundance of 9%), *Apibacter* (average relative abundance of 8.5%) and *Bacteroides* (average relative abundance of 8.2%). High relative

abundance of some genera was limited to a few samples such as *Vibrio* members in *C. julis* CSA3 (13.5%) and *Propionigenium* (14.2%) in *C. julis* CCS2. Some clusters of unsassigned taxa had high abundance in the *C. julis* from both acidified and control site. Unclassified genus of *Paludibactearaceae* family were among the most abundant genera in *C. julis* from acidified site (average relative abundance of = 9.9 %, range = 5.9- 12.6%) (Tab. 3).

Table 3. Relative abundance of the most abundant ten bacterial genera detected in fish skin associated bacterial communities

Genus	*S. scriba* 50 low pH	*S. scriba* 54 low pH	*S. scriba* 55 low pH	*S. scriba* 60 Ctrl	*S. scriba* 62 Ctrl	*S. scriba* 57 Ctrl	*C. julis* 62 low pH	*C. julis* 64 low pH	*C. julis* 67 low pH	*C. julis* 75 Ctrl	*C. julis* 78 Ctrl	*C. julis* 79 Ctrl
Unassigned	0.83	0.57	0.94	0.82	0.71	1.16	21.49	25.58	7.69	11.44	13.05	22.87
Photobacterium	29.32	25.81	13.35	14.96	8.16	8.86	0.00	0.00	1.82	0.34	0.23	0.00
Vibrio	4.50	3.21	3.38	15.66	13.44	7.85	0.00	0.09	13.56	6.51	2.17	0.08
unclassified Bacteria	2.12	1.84	2.24	2.15	2.74	2.91	10.07	8.31	10.44	8.10	7.28	9.05
Defluviitoga	9.41	8.48	10.98	9.99	10.13	11.78	0.00	0.01	1.08	1.52	0.19	0.01
unclassified												
Paludibacteraceae	0.85	0.81	1.23	0.89	1.11	1.06	11.43	12.63	5.92	4.28	7.22	13.09
Bacteroides	1.26	1.29	1.80	1.42	1.41	1.64	10.94	11.15	4.90	4.94	8.34	9.20
Apibacter	0.92	0.65	1.31	0.98	1.12	0.94	10.51	11.24	4.43	5.71	7.98	11.17
unclassified												
ClostridiaUCG014	0.51	0.39	0.71	0.56	0.74	1.08	8.25	9.54	3.37	3.91	6.36	9.14
Lactobacillus	3.03	2.46	3.43	2.70	2.84	4.88	0.18	0.34	4.81	5.74	1.58	0.56
Ligilactobacillus	1.46	1.51	1.78	1.95	1.58	1.69	0.99	1.14	6.89	6.82	3.98	1.54
Propionigenium	0.11	0.07	0.27	0.12	0.65	0.53	0.12	0.70	4.24	4.52	14.23	1.70
Enterococcus	3.29	2.57	3.95	3.14	3.31	3.29	0.00	0.01	0.86	1.18	0.18	0.03
uncultured												
Clostridium_sp.	3.09	2.79	4.43	3.52	3.78	3.30	0.00	0.00	0.00	0.00	0.00	0.00
Gilliamella	1.27	1.13	2.11	1.41	1.56	2.10	0.39	0.50	3.12	5.02	1.44	0.74
unclassified												
Muribaculaceae	2.30	2.04	2.94	2.69	2.85	3.69	0.00	0.00	0.03	0.05	0.00	0.00
unclassified												
Lachnospiraceae	1.60	1.41	1.94	1.49	1.73	2.43	0.13	0.15	1.81	2.23	0.57	0.16
Buchnera	0.13	0.15	0.25	0.20	0.17	0.22	2.49	1.97	0.71	1.07	2.72	3.28
Cetobacterium	0.00	7.30	0.03	0.71	0.24	0.29	0.08	0.37	1.35	0.19	2.03	0.39
Clostridium												
sensu_stricto_1	2.26	4.04	3.30	1.12	0.56	0.76	0.00	0.02	0.14	0.19	0.25	0.01

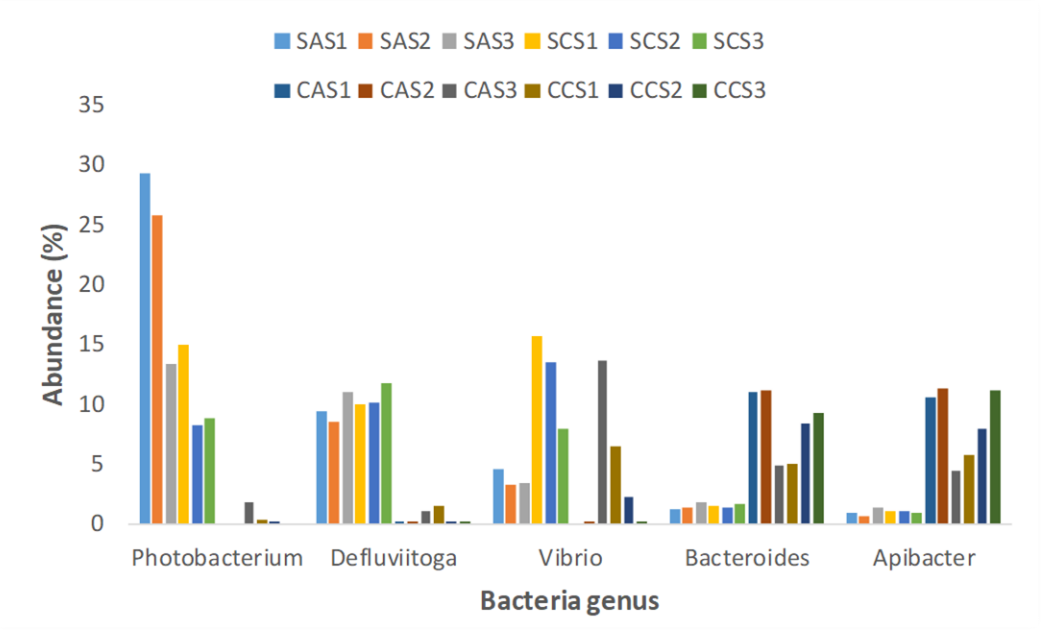

Figure 9. Selection of the five most abundant bacterial genera in each sample, obtained from the detailed analysis of the ten genera represented in the highest proportion in all analysed microbiomes (Tab. 3). The percentage of each identified genus relative to the total reads per library is presented for each sample. Different samples are represented with different colour.

1.3.3 Alpha diversity

The Simpson index showed no significant differences across all samples (Fig 10a). There was a high variation in Chao1richness and Shannon diversity between the two different species (Fig.10b). Multiple pairwise comparisons showed divergent bacterial richness between *C. julis* – *S. scriba* regardless of the site (difference between average values = 2119.6, $p < 0.05$). The Chao1 richness between *C. julis* from control and acidified sites was not significantly different ($p > 0.05$) (difference between average values = 255,6) as well in *S. scriba* in control and acidified site (difference= 283.8, $p > 0.05$).

a)

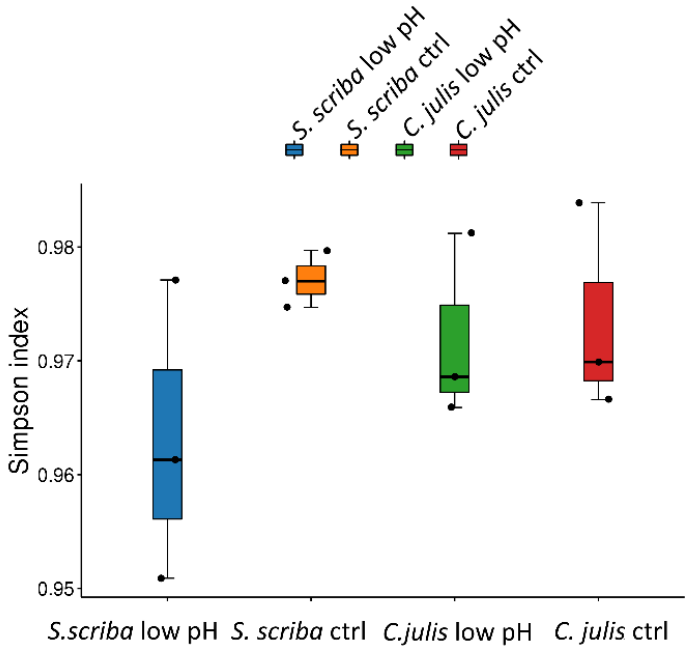

b)

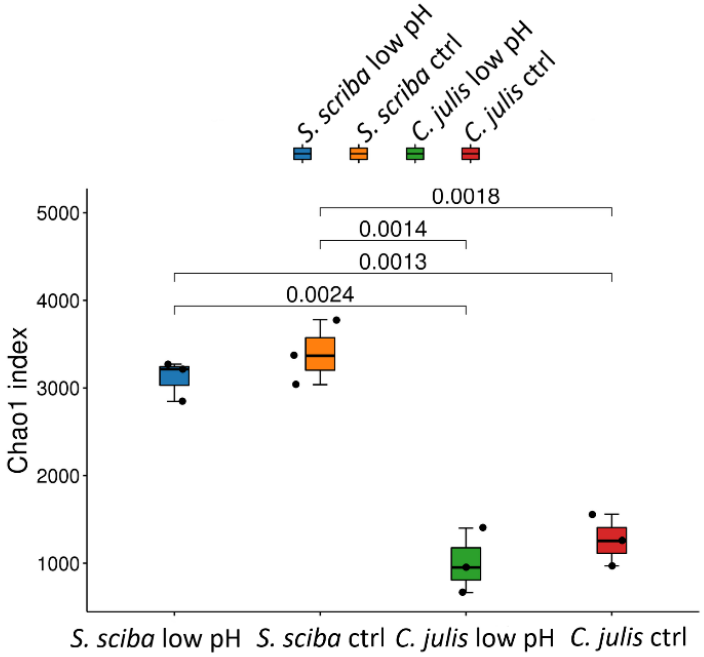

Figure 10. Boxplot presenting the median and IQR of **a)** Simpson's diversity and **b)** Chao1 diversity in *S. scriba* and *C. julis* from both low pH and control sites. Significant difference levels are also shown where p value < 0.05.

The average Shannon diversity index was around 7.26 ± 0.58 and multiple pairwise comparisons revealed that it was only significantly different between *S. scriba* from control site and *C. julis* both from control site (difference = 1.07, $p < 0.05$) and from acidified site (difference = 1.3, $p < 0.05$). The Shannon curve showed a higher number of OTU species and a higher richness of species in *S. scriba* (Fig. 11).

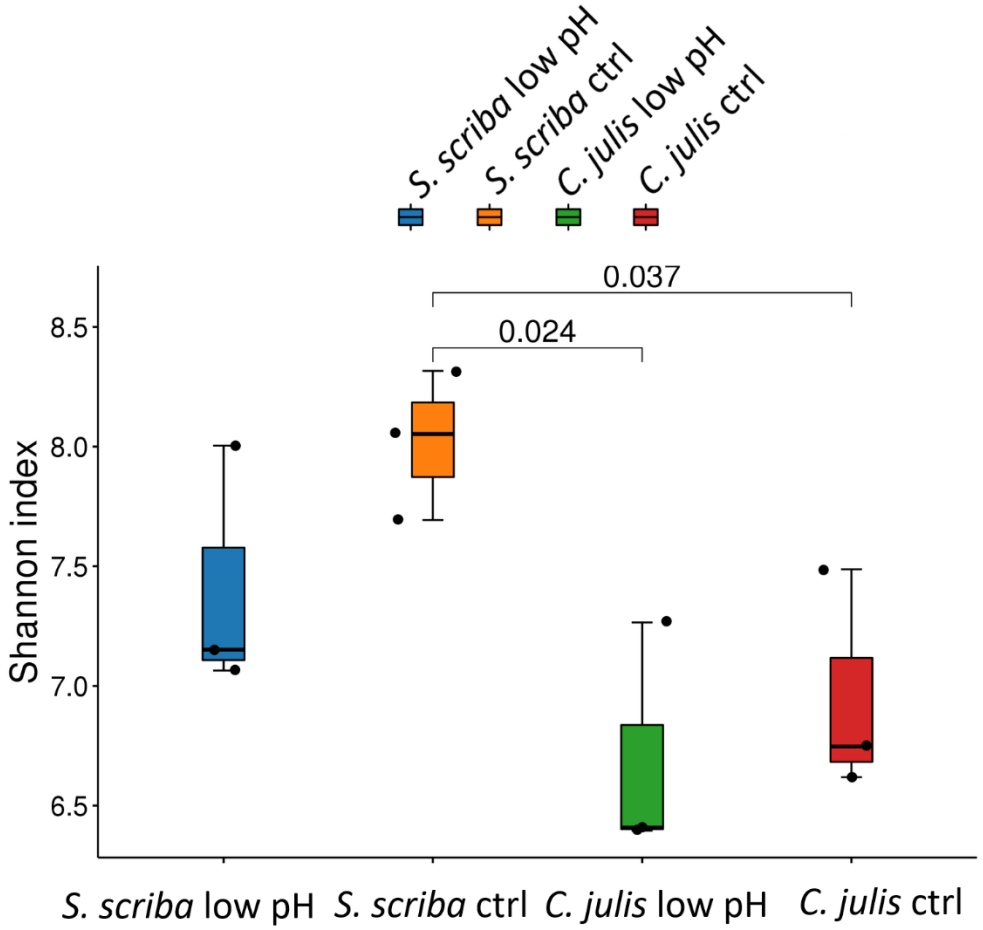

Figure 11. The alpha diversity of bacterial communities at different sampling times is measured by non-parametric Shannon index of *S. scriba* and *C. julis* from both low pH and control sites. Significant difference levels are also shown where p value < 0.05.

1.3.4 Beta diversity

Overall, a comparison of the beta diversity composition of the microbiome between samples using non-metric multidimensional scaling (nMDS) showed sample type clustering within the species (Fig. 12). The effect of species and geographical location (control and low pH) caused divergence in the microbiome. The comparison between the two different species within acidified and control site showed that *C. julis* and *S. scriba* were generally differentiated. *C. julis* from control site clustered with *C. julis* from low pH site, while in *S. scriba*, the individuals from control site were discriminated from the individuals from low pH site.

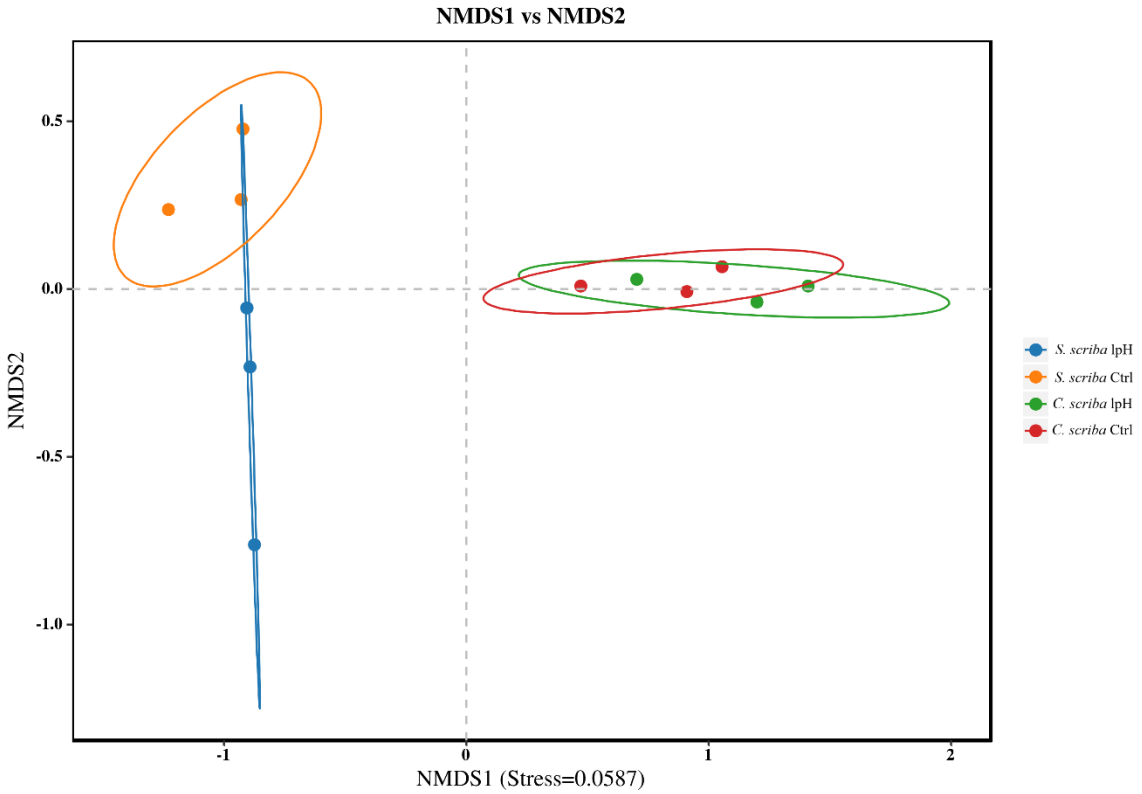

Figure 12. Nonmetric multidimensional scaling (NMDS) analysis of the two species collected in low pH and control sites. Bray–Curtis distance and data transformation were applied for the analyses.

1.3.5 Differential abundance according to sample type

The beta diversity analysis revealed distinct microbial communities between the two species and sampling sites with regard to the species *S. scriba*. Intraspecific bacterial populations were more similar between themselves compared to the other species (as is showed by the PERMANOVA analysis in Fig. 13).

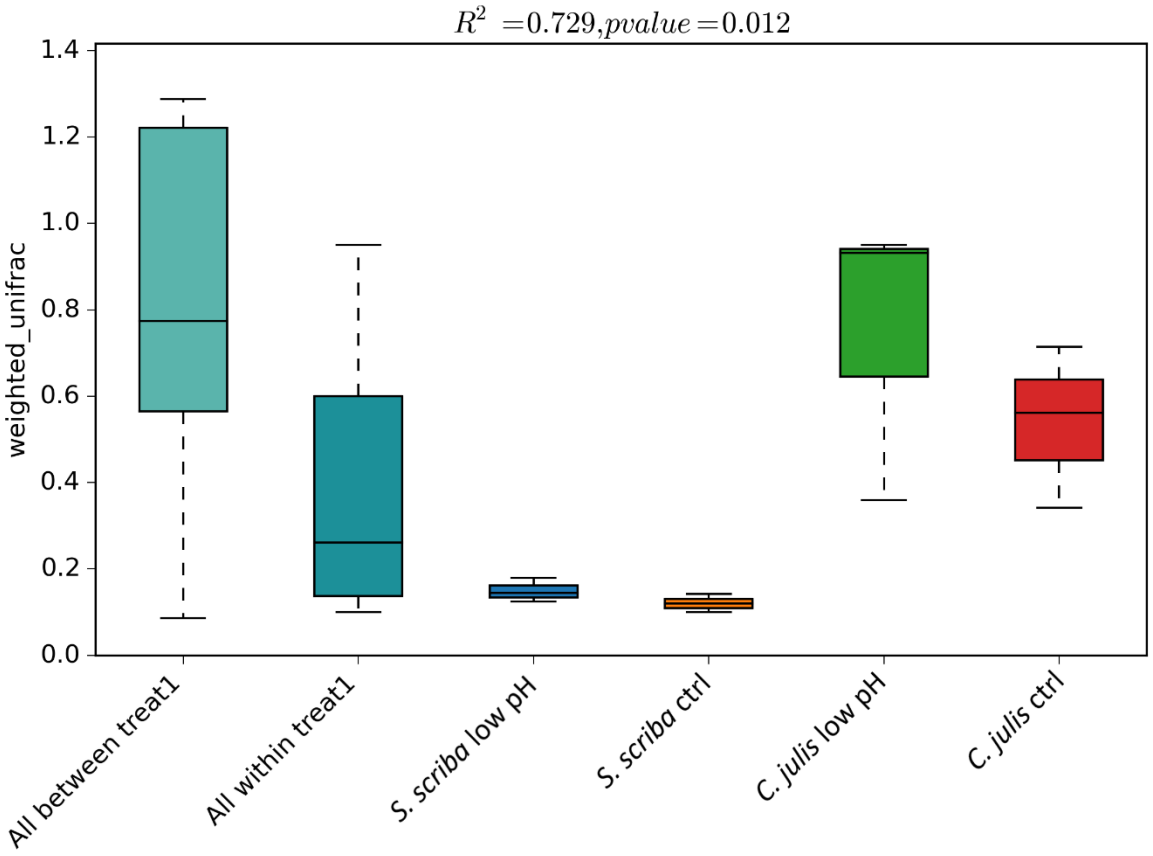

Figure 13. PERMANOVA analysis (permutations = 1000) between different types of samples groups. Above is indicated the p-value between the two species.

For example, the *Vibrionaceae* and *Petrotogaceae* families were more abundant in *S. scriba* from both sites than in *C. julis* ($p<0.05$, Fig. 14). *Paludibacteraceae*, *Weeksellaceae* and *Bacteroidaceae* were present at higher abundance in *C. julis* ($p<0.05$, Fig. 14).

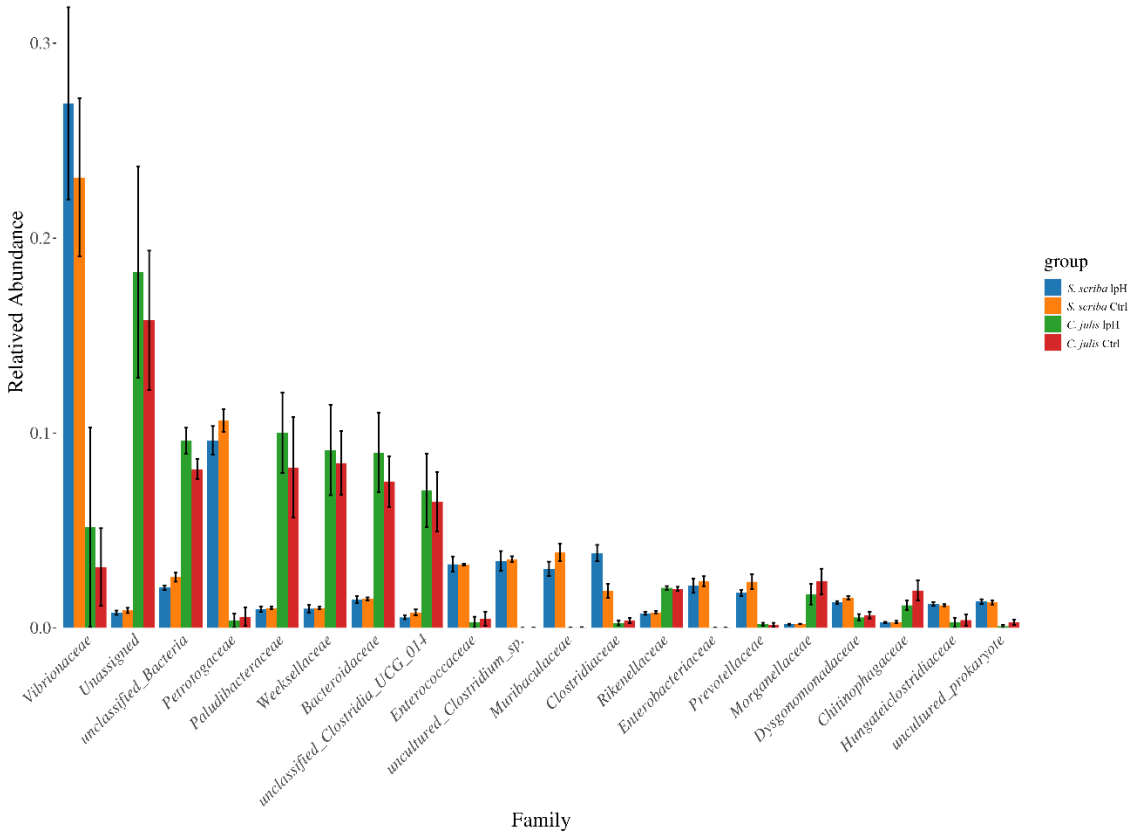

Figure 14. Relative abundances of the most abundant families in the samples grouped by species and site.

Some bacterial genera were more abundant (e.g., *Photobacterium*, *Defluviitoga*, *Vibrio*) in *S. scriba* compared to *C. julis*, while others were less abundant (e.g., *Apidebacter* and same genera from *Palidibacteraceae*) (Fig. 15). Although also in terms of genus the bacterial populations were more similar between the same species, in *S. scriba* the genus *Photobacterium* was significantly more abundant in low pH site and this was confirmed by metagenomseq.

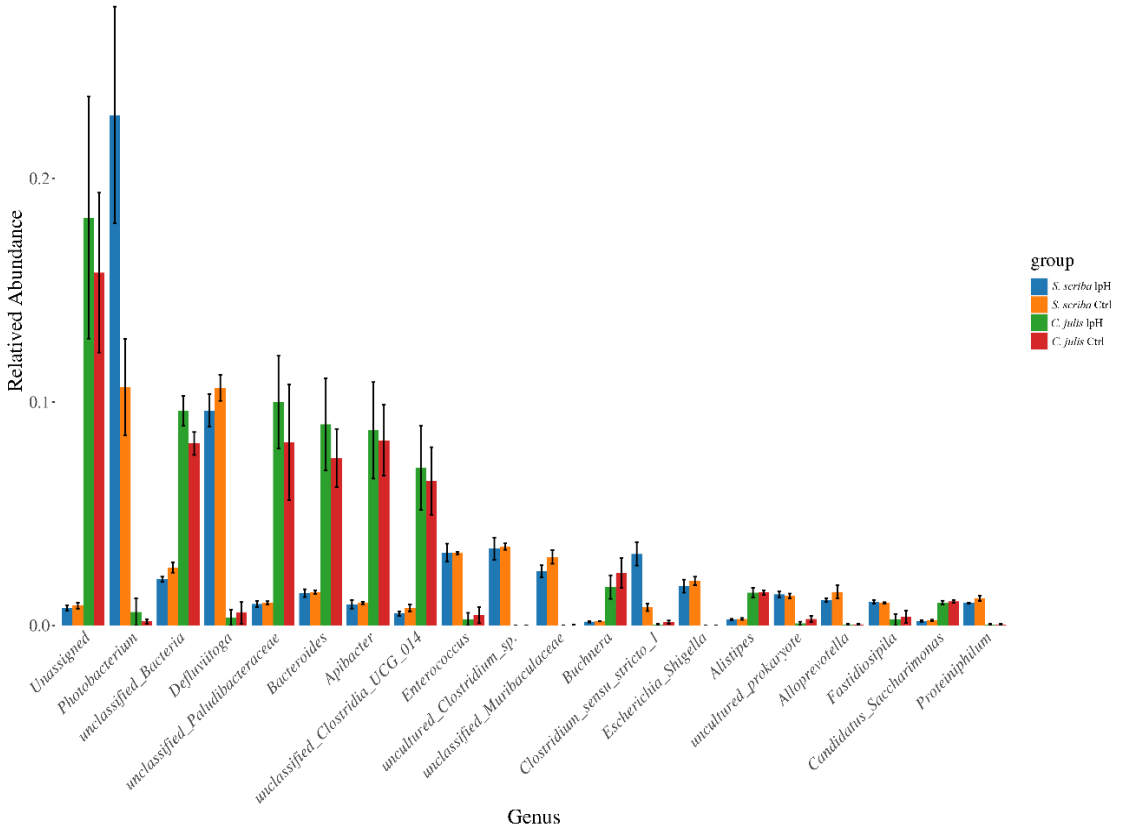

Figure 15. Relative abundances of the most abundant genus in the samples grouped by species and site.

1.3.6 Functional prediction

Common KEGG orthologs (KOs) were identified by both the RNA-seq method-edgR algorithm and metagenomeSeq used in KEGG enrichment analysis (Suppl. Table 8). Enriched KEGG pathways were identified by comparing species with each other both within the same site and between the different sites, but also by comparing the same species from different sites. Comparing the two species within the control site “Drug resistance: Antineoplastic”, “Signal transduction”, “Infectious diseases: Parasitic”, “Circulatory system”, “Digestive system”, “Cancers: Specific types”, “Excretory system”, “Neurodegenerative diseases”, “Infectious diseases: Bacterial” and “Cell motility” were enriched in *S. scriba* compared to *C. julis*, while “Nucleotide metabolism” were enriched in *C. julis*

(Fig.16). *C. julis* from control site in turn showed a great number of enriched pathways compared to *S. sciba* from control site (Fig. 16) and *S. scriba* from low pH site (Fig. 17a).

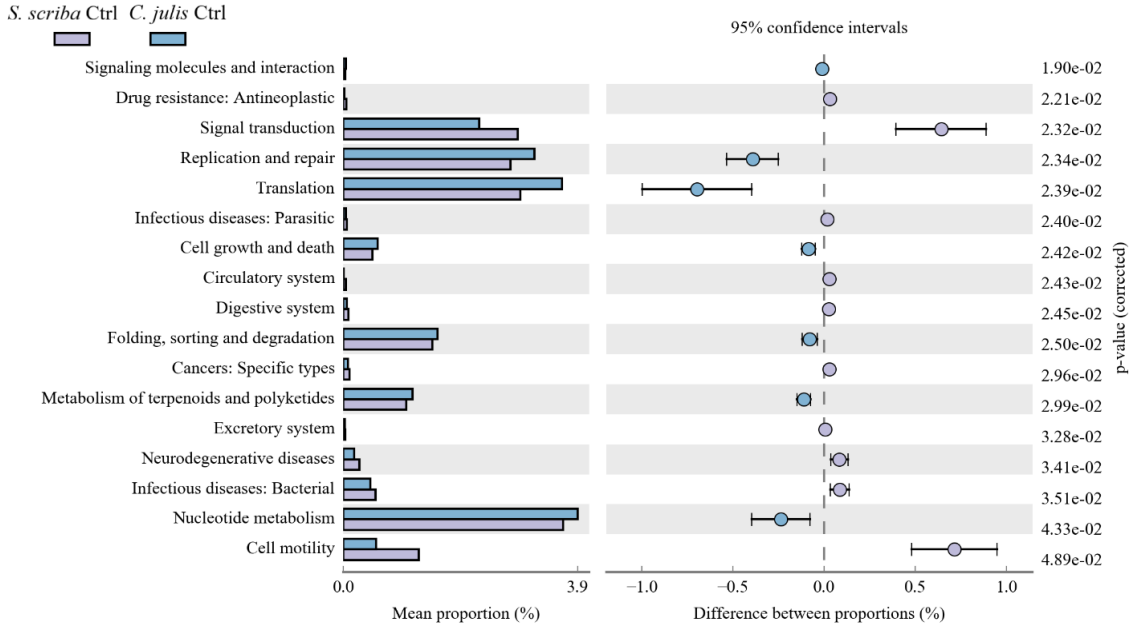

Figure 16. KEGG pathways significantly enriched in microbial communities associated to *S. scriba* and *C. julis* in the control area.

Enriched pathways in *C. julis* from control included “Signaling molecules and interaction”, “Replication and repair”, “Cell growth and death”, “Folding, sorting and degradation”, “Metabolism of terpenoids and polyketides”. “Cell motility”, “Signal transduction”, “Cancers: Specific types”, “Circulatory system, Digestive system”, “Infectious diseases: Bacterial”, “Cellular community – prokaryotes” and “Drug resistance: Antineoplastic” were enriched in *S. sciba* from low pH compared to *C. julis* from control site, while “Translation” and “Biosynthesis of other secondary metabolites” were enriched in *C. julis* from control site (Fig. 17a). “Cell motility” was enriched in *S. scriba* from low pH compared with *C. julis* from the same site (Fig. 17b) and *C. julis* from control site (Fig. 17a).

a)

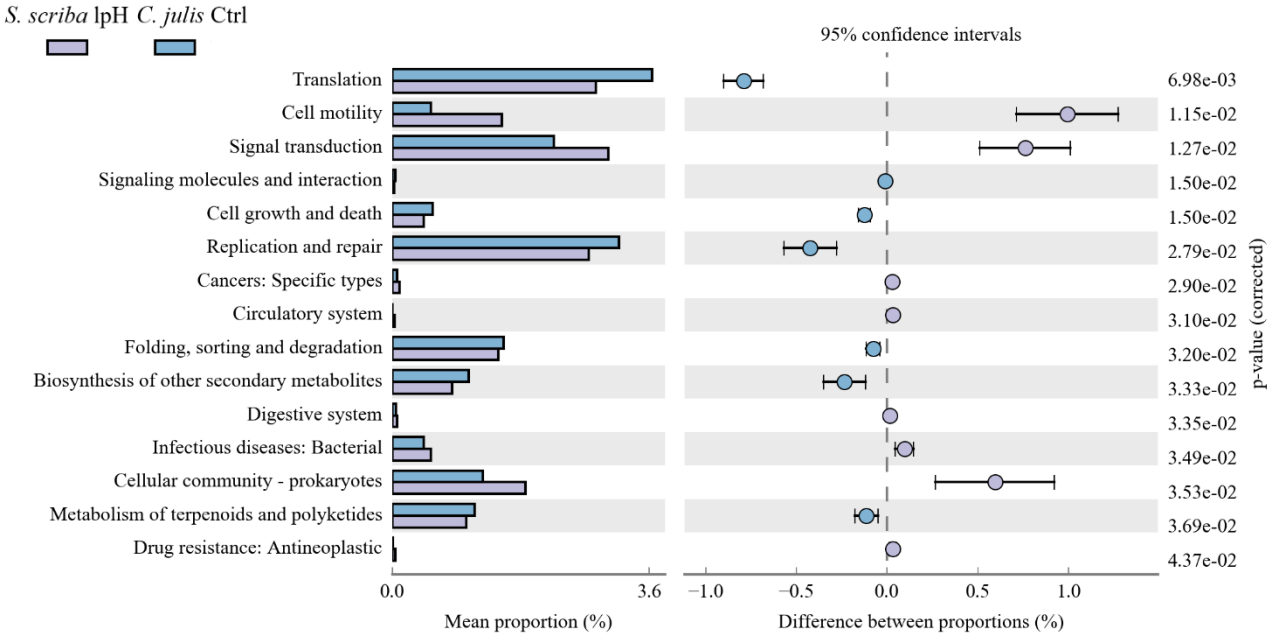

b)

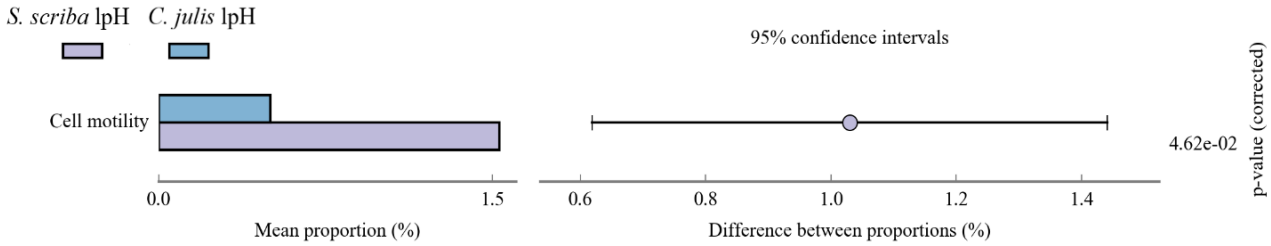

Figure 17. KEGG pathways significantly enriched in microbial communities associated to **a)** *S. scriba* from low pH site and *C. julis* from control site; **b)** *S. scriba* and *C. julis* in low pH site.

1.4 Discussions

The initial project was to investigate the microbiome of the skin and gills of *C. julis* and *S. sciba* living in two different natural environments and characterized by different pH conditions. The aim was to identify a core bacterial community in both tissues and for both species with the purpose to observe how the microbial community of skin and gills changed in the two species and at the two sites. However, to date, sequencing and bioinformatics have only been performed on skin DNA.

The present 16S rRNA gene metabarcoding study shows that there the significant differences in microbial communities between *C. julis* and *S. scriba* were most specie-specific than correlated to the pH conditions. Anyway, the *S. scriba* species, seems to be more sensitive to the acidified pH conditions.

The most abundant and common phyla detected across all skin samples were *Firmicutes, Proteobacteria* and *Bacteroidota* that may be considered core or common bacterial phyla in fish since they have also been identified among the topmost bacterial phyla in other studies of fish microbiomes.

1.4.1 Microbiome' species richness and diversity

Species richness and diversity of the skin microbiomes were higher in *S. scriba* than in *C. julis.* A higher variation in Chao1 richness and Shannon diversity was reported between the two different species. Differences in microbial communities were revealed also by the beta diversity analysis. Although the phyla *Proteobacteria, Firmicutes, Bacteroidota* were detected for both *S. sciba* and *C. julis*, they were differently represented in the total microbial communities between the two species. *Proteobacteria* were the most abundant phylum in *S.*

scriba and significantly higher rather than in *C. julis*, whose top phylum was represented by *Bacteroidota*. The phyla *Thermotogota* was highly represented in *S. sciba* and almost absent in *C. julis.* The families *Vibrionaceae* and *Petrotogaceae* were higher in *S. sciba* compared to *C. julis* which presented on the other hand a higher abundance of *Paludibacteraceae*, *Weeksellaceae* and *Bacteroidaceae.* The higher bacterial richness in *S. scriba* was prominent also at genus level, in particular *Photobacterium*, *Defluviitoga* and *Vibrio* were more abundant compared to *C. julis*. This may indicate who are more vulnerable to disease given the nature of *Vibrio* and *Photobacterium.* Indeed, *Apidebacter* and same genera from *Palidibacteraceae* were more abundant in *C. julis.*

1.4.2 The effect of pH on microbiome

No significant variations in Chao1 richness were detected for both *S. scriba* and *C. julis* specimens between the two different sites. The non-metric multidimensional scaling (nMDS) and the beta diversity analysis revealed some significant differences within the species *S. scriba* from the two different sites. The results revealed a higher relative abundance of the phylum *Proteobacteria* in *S. sciba* living under low pH conditions than under normal conditions. These results are in line with those obtained by (Sylvain et al. 2016) and are further confirmation of the opportunistic nature of *Proteobacteria*, as already documented by Shin, Whon, e Bae (2015) and (Laplante, Sébastien, e Derome (2013). The higher abundance of the genus *Photobacterium* is in *S. scriba* exposed to low pH conditions is most likely explained by its presence proliferation under ocean acidification (Ng e Chiu 2020). Surprisingly and in contrast to other studies that display how the abundance of *Vibrio* sp. was increased under acidified conditions at least in *S. scriba*, specimens that were naturally exposed to low pH, the genus *Vibrio* was significantly less abundant compared to the control site.

These results suggest an increased sensitivity of the species *S. scriba* under acidifying conditions and a species-specific response. Additionally, *Vibrio* sp. and *Photobacterium* sp. are known to play a critical role in fish diseases, causing vibriosis and pasteurellosis, two of the most common and severe illnesses in global marine aquaculture. For instance, *P. toruni* and *P. malcacitanum* have been found to be pathogenic to red banded seabream in Southern Spain (A. M. Labella et al. 2018; A.M. Labella et al. 2020), while *Vibrio harveyi* and *V. alginolyticus* are commonly isolated from diseased fish in the initial stages of farming (Ina-Salwany et al. 2019).

1.4.3 Further analysis

Next aim is to integrate the data obtained on the skin microbiome with a view to conduct a comprehensive molecular study. The specific tasks are the microbiome determination from other tissues (gills) and the evaluation of potential changes in gene expression in gills tissue. In order to achieve these goals, further DNA extractions have already been carried out from the gills to sequence 16S rRNA and determine potential microbiome changes in this anatomical location as well. In addition, RNA was extracted by the gills samples to carry out limited RNA seq and design quantitative PCR reaction for the analysis on gene expression. The final goal will be to evaluate possible changes in the microbiome for other tissues outside the skin and to assess whether acidified conditions determine changes in the host gene expression.

2. LONG-TERM EFFECTS OF HIGH CO_2 LEVEL EXPOSURE ON MINERALOGICAL FEATURES OF FISH BONES

2.1 Introduction

To date, climate change research has primarily focused on organisms with calcium carbonate biological structures. However, more research is needed on calcium phosphate minerals produced by small and large marine organisms (elasmobranchs, teleosts, and marine mammals) to understand how they will react to different environmental conditions in future oceans.

Fish built biological mineralized structure in hydroxylapatite (HAP), a calcium phosphate mineral with a very specific structure and composition. HAP features naturally change with time (mineral becomes more crystalline, its PO_4^{2-} content increases and its content of carbonate and acid phosphate decreases) but also can be altered by environmental factors resulting in an abnormal composition (Boskey e Mendelsohn 2005; Glimcher 1998). Although fish have been considered able to cope with extra-cellular acidosis thanks to their acid-base regulation (Melzner et al. 2009), some effect on their mineral structure was showed after a low pH exposition. The natural exposition of some fish species to natural CO_2 emissions and reduced pH leads a significant change in otoliths elemental and isotopic signatures showing likewise their potential application as natural tags (Mirasole et al. 2017). While other studies show how otoliths size and density increased in fish exposed to low pH conditions with the potential to substantially influence the dispersal, survival, and recruitment of a pelagic fish species (Mirasole et al. 2017; Bignami et al. 2013; Checkley et al. 2009). Another fish body part made of calcium phosphate minerals impacted by the corrosive effect of acidified seawater are the denticles. In demersal shark *Haploblepharus edwardsii* it was observed the denticles corrosion as a result of chronic exposure to low pH (Dziergwa et al. 2019). Although OA appear to affect negatively marine organisms, in Port

Jackson shark, *Heterodontus portusjacksoni* the fluorapatite ($Ca_5(PO_4)_3F$) composition of the teeth changed increased fluoride content under ocean acidification that was associated with increased crystallinity by suggesting an adaptive response considering that the teeth were more resistant to corrosion (Leung et al. 2022).

Although fishbone has already resulted in excellent environmental bio-indicators showing as heavy metal contamination can alter the biochemical and mineral contents in fishbone (Scopelliti et al. 2015), there are no knowledge about the response to this structure to OA. While the direct effects of OA on skeletal development are not expected (P. Munday et al. 2011a) under acidified and hypercapnic conditions, fish compensate for acidosis by increasing the plasma bicarbonate and non-bicarbonate buffer levels (a process known as acid–base regulation) (Brauner e Baker 2009), and it has been suggested that this buffering capacity may have the side effect of accumulating phosphate in blood with possible interference on skeletal development (Di Santo 2019).

Spectroscopic methods enable the measurement of physicochemical changes in minerals caused by mechanical testing (Ager et al. 2005; Akkus, Adar, e Schaffler 2004; A. Carden et al. 2003), age-related modifications (Ager et al. 2005; Akkus et al. 2003; L. M. Miller et al. 2007), and pathological or treatment-related changes (Boskey e Mendelsohn 2005; Angela Carden e Morris 2000; Fratzl et al. 2004; L. M. Miller et al. 2004). By combining X-Ray Diffraction (XRD), Fourier Transform Infrared Spectroscopy (FT-IR) and ICP-OES spectroscopy we wanted to investigate the fishbone mineral composition of two different fish species that differ in age and exposure conditions. There were three different goals:

1) evaluate how mineral composition might change within the same species as the fish gradually become older;
2) evaluate any potential difference between specimens of the same age but different species and exposure conditions;

3) develop a method and provide useful information on the correlation between skeletal composition and age for the two species: *C. julis* and *S. scriba*.

Otoliths were analysed to determine fish age and then to assign specimens to an age range. Otoliths, indeed, are a valuable tool for several scientific approaches (species identification - Tuset, Rosin, e Lombarte 2006; Jawad 2007, population studies Stransky et al. 2008, ecomorphological studies - Volpedo 2003, determining prey identity in feeding studies - Waessle, Lasta, e Favero 2003; Tarkan et al., 2007 including fish ageing - Pino et al. 2004; Do, Gronkjaer, e Simonsen 2006.

2.2 Materials and Methods

2.2.1 Sampling and analytical methods

For mineralogical analysis, a total of 104 specimens were collected in the control site and in a low pH site. Between August 2022 and May 2023, 28 *S. scriba* and 41 *C. julis* were sampled from a low pH site (mean pH = 7.21 ± 0.34) on the north side of the Castello Aragonese (40°43’55” N, 13°57’51” E) while 16 *S. scriba* and 19 *C. julis* were collected from one ambient pH (mean pH = 8.1 ± 0.02) site located 2 Km far away from Castello Aragonese vents, in front of S. Pietro beach (40°44'48"N 13°56'40"E) used as control station. Specimens were collected during fishing sessions conducted in snorkelling by hand line with natural bait. Each specimen was measured to the nearest mm (Standard Length, SL; Total Length, TL) and weighed to the nearest 0.1 g (Total Weight, TW). Individuals were dissected to collect otoliths and skeleton. From each fish, the sagittal otolith pair was removed by opening the otic bulla under the operculum, cleaned and

stored dry. Sagittal otoliths were used for age determination, whereas the whole skeleton was prepared for mineralogical analysis (see details in the following paragraphs). Age was determined in order to correlate it with the mineral characteristics of the skeleton. then only the most abundant age classes were used for spectroscopic analysis, with the goal of ensuring a suitable number of replicates. Thus only 22 *C. julis* and 28 *S. scriba* from both sites were analysed out of a total of 104 individuals.

2.2.2 Age determination

The sagittal otoliths were used to determine fish age (Gordoa, Molí, e Raventós 2000). They were removed, cleaned, washed with distilled water to remove organic tissues, dried and stored in labelled plastic vials. Age was estimated from 60 *C. julis* and 44 *S. scriba*.

Whole otoliths were immersed in a glycerol – ethanol (1:1) clearing solution to enhance the visualization of annual increments during the reading (Alonso-Fernández et al. 2011; Alós et al. 2010). The otoliths were positioned in a glass petri dish with the sulcus acusticus down, using a stereo microscope (Stemi 508 Microscopy with Axiocam 305 colour) under reflected light against a black background. An otolith was discarded because it was unreadable.

According to current knowledge, the period of maximum settlement (the movement of a juvenile fish from the planktonic to the benthic environment) is the beginning of August for *C. julis* (García-Rubies e Macpherson 1995) and August – September for *S. scriba* (Biagi, Gambaccini, e Zazzetta 1998).

Considering that the duration of the larval stage of life varies between one and two months, it was assumed a birthdate in June/July for both *C. julis* and *S. scriba*.

For these reasons, according to (Carbonara e Follesa 2019) a theoretical birth date of 1 July was set for these species (fish with a spawning period concentrated in late spring/summer/early autumn).

Translucent bands (hyaline zones) that extended around the whole diameter of the otolith were identified as annuli, and the total number of these bands was recorded. According to the ageing scheme (Carbonara e Follesa 2019) (Tab.4) for the specimens caught in the first part of the year (winter/spring) when the translucent ring on the edge was present this was not counted as an annual ring as the birth date has not yet passed. Thus the age was estimated as the number of translucent rings, including the edge, minus 0.5.

Table 4. Ageing scheme for species with a birth date of 1 July.

Date capture	Otolith edge	Age
1 January-30 June	Transparent	N - 0.5
1 July-31 December	Opaque	N

Note: N is the number of translucent rings, including those that might be visible on the edge.

In the specimens caught in the second part of the year (summer/autumn), when an opaque ring was present on the otolith edge, the age was equal to the number of translucent rings (Tab.5).

Table 5. Ageing scheme for species with a birth date of 1 July.

Months	Jan	Feb	Mar	Apr	May	Jun	July	Aug	Sep	Oct	Nov	Dec
Deposition pattern	T/O	T	T	T	T	O/T	O/T	O	O	O	O	T/O
Capture date												
Age with edge T	N-0.5	N-0.5	N-0.5	N-0.5	N-0.5	N-0.5	N					N-1
Age with edge O	N+0.5					N-0.5	N	N	N	N	N	N

Note: N is the number of winter rings (translucent); T = transparent edge, O = opaque edge.

A distinctive opaque core consist-ing was observed in all the examined otoliths. this more opaque central zone can be considered on the basis of the daily ring

count, corresponding to the planktonic larval duration (PLD) (N. e E. 2001; Fontes et al. 2010; Škeljo et al. 2012).

The PLD zone is followed by the narrow translucent ring (F), an opaque O1 and another translucent T1 ring all formed within eight months of birth. The second opaque ring (O2), much larger than the first, corresponds approximately to the first year of life (Škeljo et al. 2012). Thus fish age was estimated by counting opaque annual rings, starting with the second one. Images were employed for age reading since their size and quality made interpreting the zoning pattern simpler than direct microscopy views (Fig.19).

Figure 19. *Coris julis*. Sagittal otolith of a 4-year-old specimen, in-dicating: planktonic larval duration (PLD), "false" translucent ring (F), four translucent rings (T1-T4) and five opaque rings (O1-O5); second opaque ring (O2) corresponds to the first year of age.

2.2.3 Analytical methods

Fifty-nine *C.julis* and 44 *S. scriba* were initially prepared for the XRD. A number of vertebrae were removed from the stripped skeleton. After an initial clean-up trying to remove as much excess non-bone tissue as possible, vertebrae were freeze-dried (Alpha 1-2 LDplus, Martin-Christ) for at least 48 hours. Afterwards, the samples were washed with acetone in an ultrasonic bath for 60 min to remove collagens, fats and other impurities (Scopelliti et al. 2015; Juraida et al. 2011). All vertebrae were ground to a fine powder using a tissue lyser (Mixer Mill MM400). Finally, only 22 *C. julis* and 28 *S. scriba* were subjected to XRD analysis at the laboratories of the University of Palermo (under the supervision of prof. Giovanna Scopelliti) as they belonged to the size classes that were to be assessed. Specimens within the following size classes were used: 2, 3 and 4 years for *C. julis* and 1,2,3 and 4 years for *S. scriba*. Each size class consisted of at least 3 replicates.

X-Ray Diffraction (XRD) is a standard method for investigating crystal structure and atomic spacing. XRD examination was done on fishbone-powered samples using a Philips PW14 1373 with Cu Ka radiation filtered by a mono-chromator crystal. The step size was 1/2 °2θ and the time/step was 2 s. The angle of diffraction was 20-60 °2 θ (Scopelliti et al. 2015).

2.3 Results

2.3.1 Age determination

Otoliths from 44 *S. scriba* and 59 *C. julis* specimens were analysed for age determination. Up to seven marks, assumed to be annuli, were visible in the otoliths. Age classes in the otolith sample ranged from 1+ to 5 years for *C. julis*

and from 1 to 7 for *S. scriba*; dominant age classes were 2 and 3 for *C. julis* and 1 and 2 for *S. scriba* (Tab. 4a and 4b).

Table 6. Age-length key for **a)** *S. scriba* and **b)** *C. julis.*

a)

Total	Age (years)						
length (cm)	1	2	3	4	5	6	7
10	1						
12	1	1					
13		4					
14	1	8	2	1			
15	2	7	4	3			
16						1	1
17				2			
18						1	
19					1		1
22						1	
n	5	20	6	6	1	3	2
TL Mean	13,1	14,1	14,7	15,2	19,0	16,9	17,3

b)

Total	Age (years)				
length (cm)	1	2	3	4	5
10	3				
11		3			
12		9	1		
13		6	9		
14		8	3	2	
15			4	1	
16			4	2	
17			1		
19				1	1
20				1	
n	3	26	22	7	1
TL Mean	10.0	12.8	14.1	16.4	19.2

2.3.2 X-ray diffraction

Mineral crystallinity is defined as the degree of order in a solid and the width of an X-ray diffraction line represents a measure of the average bone crystallite size, perfection and ordering (crystallinity) in a particular diffraction plane (Cullity, 1967), where narrower linewidths indicate increased crystallinity. The (002) reflection, which offers an indicator for c-axis crystal size, is perhaps the simplest approach to assess the crystallinity of bone mineral (Alvarez-Lloret et al., 2006; (L. M. Miller et al. 2001). This reflection was used in this study to construct the Crystallinity Index (CIXRD) as the inverse ratio of the full width at half maximum (FWHM; Farlay et al. 2010). Data obtained for *C. julis* were in the range of 1.2 – 1.8 °2ϑ while for *S. scriba* were in the range of 1,23 – 1,78 °2ϑ (Tab.7).

Table 7. correlation of site age and C.I.

Species	Site	Age	CI
C. julis	Ctrl	2	1.27
C. julis	Low pH	2	1.35
C. julis	Ctrl	3	1.46
C. julis	Low pH	3	1.47
C. julis	Ctrl	4	1.59
C. julis	Low pH	4	1.69
Species	Site	Age	CI
S. scriba	Ctrl	1	1.49
S. scriba	Low pH	1	1.66
S. scriba	Ctrl	3	1.38
S. scriba	Low pH	3	1.32
S. scriba	Ctrl	4	1.46
S. scriba	Low pH	4	1.56

In general, for *C. julis*, crystallisation index values increase with age. Between the two sites (control and low pH), there were no significant differences for *C. julis* in the three-year-old age groups. Considerably higher values were shown by 4 and

two-year-old *C. julis* in the low pH site than in the control site (Fig.20a). The values for *S. scriba* show no particular differences between the different age groups however, in individuals from the low pH site, age classes 1 and 4 had higher CI values than individuals of the same age but from the control site (Fig.20b).

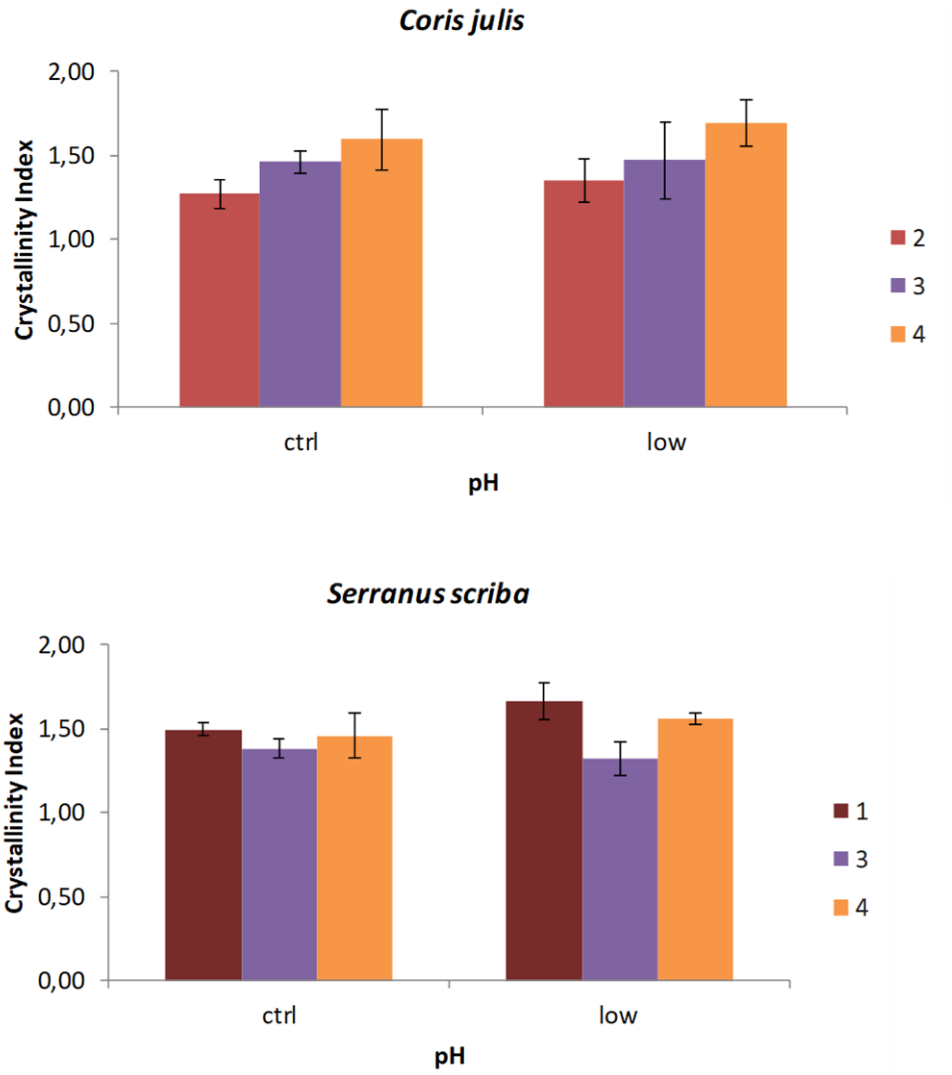

Figure 20. Mean (±SD) of skeleton C.I. of **a)** *C. julis* and **b)** *S. scriba* among the age in the two different site.

2.4 Discussion

The initial project involved investigating the mineral features of the skeleton of *C. julis* and *S. scriba* across the age classes and living in two different natural environments with different pH conditions. One of the objectives was to find the correlation between age and the state of maturation of the vertebrae and to examine whether low pH conditions can interfere with skeletal maturation in teleosts.

The methodological approach envisaged in the initial project involved combining different spectroscopic techniques such as XR-Diffraction, FT-IR Spectroscopy and ICP-OES analyses. The results obtained are the result of a preliminary analysis as to date only XRD analyses have been carried out on the skeleton samples. The diffractometric analysis revealed that the main mineral component of skeleton tissues is the HAP, which is an end-member of the apatite group and is of scientific interest due to its wide range of applications in (environmental) mineralogy, geology, biomineralization, medicine, and biomaterials. The HAP is an end-member of the apatite group with general formula $Ca_{10}(PO_4)_6(OH)_2$ (Wopenka e Pasteris 2005). It has sites for ion attachment that can be occupied by different elements with different ionic charge (Pan e Fleet 2002; Piccoli e Candela 2002). The ionic substitutions into the HAP structure will result in slight structural changes and they may vary as a function of age. These changes may be quantified by measuring the skeleton mineral features, such as the crystallinity index (C.I.), the mineral maturity (Min. Mat.), and the phosphate/carbonate content (Phosp/Carb). One of the key points of this project was to evaluate if variations in the chemical composition and bone mineralogy are only due to normal bone development related to biological growth or if they are also influenced by trace element substitution, like in natural high CO_2 areas such as Castello Aragonese. The results indicated that the XRD reflection (002) showed a narrower peak in correspondence with an increase in crystallization degree. As expected, in *C. julis*

the crystallization degree seems to be correlated with the age as this increases with age. The clearest change observed is, indeed, an increase in bone mineral crystallinity with ageing (e.g., Alvarez-Lloret et al., 2006). However, in *S. sciba* samples the mineral parameters are uncorrelated with ageing and show dissociation values, especially for the 1-year age group. The higher crystallisation index in all the age classes analysed for *C. julis* and of two out of three age classes for *S. scriba* at the low pH site compared to the control site is in line with the results found by Di Santo (2019), confirming that acidification may play a significant role in other physiological processes related to mineralization.

However, a better understanding of physiological responses from the perspective of mineralogical structures in fish will require further investigation. To pursue this goal Fourier transform infrared spectroscopy (FT-IR) and ICP-OES analyses will be performed to evaluate other mineral features, such as carbonate/phosphate mineral content and chemical composition in fishbone.

General conclusions

This study underscores the rilevant role of CO2 vents as natural laboratories for testing ecological hypotheses regarding the effects of ocean acidification on marine organisms. The findings suggest that CO2 vents can be utilized as unique environments to investigate the biological impacts of decreased pH levels, offering valuable insights into the resilience and adaptability of marine life.

The microbiome investigation on the studied fish species identity had a more pronounced influence on microbial community composition than the surrounding environmental conditions. Specifically, the microbiota of *S. scriba* is richer and more diverse than that of *C. julis,* indicating that different species may have evolved distinct microbial associations that could influence their health and ecological roles.

Furthermore, our results suggest a species-specific response to low pH conditions, with *S. scriba* showing a marked increase in the abundance of Proteobacteria and Photobacterium in acidified environments. In contrast, the relative decrease in Vibrio abundance points to potential shifts in microbial dynamics under stress, which could have implications for disease susceptibility and overall fish health.

Although no statistical analysis were conducted, the comparative mineralogical analysis revealed that the C.I. measured in both *C. julis* and *S. scriba* were slightly higher under low pH conditions than control, these findings align with previous studies suggesting that acidification may influence mineralization processes Di Santo (2019). Despite the absence of malformations, the subtle changes in the C.I. could reflect underlying physiological adaptations or stress responses that warrant further investigation.

Differences in C.I. index seen in fish exposed to high pCO2 levels could could suggest interference with neural activity or a physiological response with uncertain ecological implications. These initial observations emphasize the

complexity of the responses to acidification, highlighting the need for a multifaceted approach in future studies to fully elucidate the effects of pH on fish physiology and ecology.

In conclusion, while our study utilized a limited methodological framework, the preliminary findings offer crucial insights into fish physiology under high pCO2/low pH conditions. This research not only emphasizes the significance of shallow volcanic vents as natural experimental sites but also points to the need for further studies that integrate diverse methodologies to comprehensively understand the ecological and physiological implications of ocean acidification.

Future research should aim to explore the long-term impacts of acidification on marine ecosystems, including the potential for shifts in community structure and function. Additionally, examining the interplay between microbial communities and their host species could unveil new dimensions of resilience in marine organisms facing climate change.

Bibliography

Ager, J. W., R. K. Nalla, K. L. Breeden, e R. O. Ritchie. 2005. «Deep-Ultraviolet Raman Spectroscopy Study of the Effect of Aging on Human Cortical Bone». *Journal of Biomedical Optics* 10 (3): 034012. https://doi.org/10.1117/1.1924668.

Akkus, Ozan, Fran Adar, e Mitchell B. Schaffler. 2004. «Age-Related Changes in Physicochemical Properties of Mineral Crystals Are Related to Impaired Mechanical Function of Cortical Bone». *Bone* 34 (3): 443–53. https://doi.org/10.1016/j.bone.2003.11.003.

Akkus, Ozan, Anna Polyakova-Akkus, Fran Adar, e Mitchell B Schaffler. 2003. «Aging of Microstructural Compartments in Human Compact Bone». *Journal of Bone and Mineral Research* 18 (6): 1012–19. https://doi.org/10.1359/jbmr.2003.18.6.1012.

Alonso-Fernández, Alexandre, Josep Alós, Amalia Grau, Rosario Domínguez-Petit, e Fran Saborido-Rey. 2011. «The Use of Histological Techniques to Study the Reproductive Biology of the Hermaphroditic Mediterranean Fishes *Coris Julis* , *Serranus Scriba* , and *Diplodus Annularis*». *Marine and Coastal Fisheries* 3 (1): 145–59. https://doi.org/10.1080/19425120.2011.556927.

Alós, Josep, Miquel Palmer, Alexandre Alonso-Fernández, e Beatriz Morales-Nin. 2010. «Individual Variability and Sex-Related Differences in the Growth of Diplodus Annularis (Linnaeus, 1758)». *Fisheries Research* 101 (1–2): 60–69. https://doi.org/10.1016/j.fishres.2009.09.007.

Ángeles Esteban, María, e Rebeca Cerezuela. 2015. «Fish Mucosal Immunity: Skin». In *Mucosal Health in Aquaculture*, 67–92. Elsevier. https://doi.org/10.1016/B978-0-12-417186-2.00004-2.

Baumann, Hannes, Stephanie C. Talmage, e Christopher J. Gobler. 2012. «Reduced Early Life Growth and Survival in a Fish in Direct Response to Increased Carbon Dioxide». *Nature Climate Change* 2 (1): 38–41. https://doi.org/10.1038/nclimate1291.

Biagi, Franco, Silvia Gambaccini, e Massimo Zazzetta. 1998. «Settlement and Recruitment in Fishes: The Role of Coastal Areas». *Italian Journal of Zoology* 65 (sup1): 269–74. https://doi.org/10.1080/11250009809386831.

Bignami, Sean, Ian C. Enochs, Derek P. Manzello, Su Sponaugle, e Robert K. Cowen. 2013. «Ocean Acidification Alters the Otoliths of a Pantropical Fish Species with Implications for Sensory Function». *Proceedings of the National Academy of Sciences* 110 (18): 7366–70. https://doi.org/10.1073/pnas.1301365110.

Bolger, Anthony M., Marc Lohse, e Bjoern Usadel. 2014. «Trimmomatic: A Flexible Trimmer for Illumina Sequence Data». *Bioinformatics* 30 (15): 2114–20. https://doi.org/10.1093/bioinformatics/btu170.

Bolyen, Evan, Jai Ram Rideout, Matthew R Dillon, Nicholas A Bokulich, Christian Abnet, Gabriel A Al-Ghalith, Harriet Alexander, et al. 2018. «QIIME 2: Reproducible, Interactive, Scalable, and Extensible Microbiome Data Science». https://doi.org/10.7287/peerj.preprints.27295v2.

Boskey, Adele, e Richard Mendelsohn. 2005. «Infrared Analysis of Bone in Health and Disease». *Journal of Biomedical Optics* 10 (3): 031102. https://doi.org/10.1117/1.1922927.

Branch, Trevor A., Bonnie M. DeJoseph, Liza J. Ray, e Cherie A. Wagner. 2013. «Impacts of Ocean Acidification on Marine Seafood». *Trends in Ecology & Evolution* 28 (3): 178–86. https://doi.org/10.1016/j.tree.2012.10.001.

Brauner, C.J., e D.W. Baker. 2009. «Patterns of Acid–Base Regulation During Exposure to Hypercarbia in Fishes». In *Cardio-Respiratory Control in Vertebrates*, a cura di Mogens

L. Glass e Stephen C. Wood, 43–63. Berlin, Heidelberg: Springer Berlin Heidelberg. https://doi.org/10.1007/978-3-540-93985-6_3.

Brugman, Sylvia, Wakako Ikeda-Ohtsubo, Saskia Braber, Gert Folkerts, Corné M. J. Pieterse, e Peter A. H. M. Bakker. 2018. «A Comparative Review on Microbiota Manipulation: Lessons From Fish, Plants, Livestock, and Human Research». *Frontiers in Nutrition* 5 (settembre):80. https://doi.org/10.3389/fnut.2018.00080.

Butt, Robyn Lisa, e Helene Volkoff. 2019. «Gut Microbiota and Energy Homeostasis in Fish». *Frontiers in Endocrinology* 10 (gennaio):9. https://doi.org/10.3389/fendo.2019.00009.

Caldeira, Ken, e Michael E. Wickett. 2003. «Anthropogenic Carbon and Ocean pH». *Nature* 425 (6956): 365–365. https://doi.org/10.1038/425365a.

Caldeira, K. 2005. «Ocean Model Predictions of Chemistry Changes from Carbon Dioxide Emissions to the Atmosphere and Ocean». *Journal of Geophysical Research: Oceans* 110 (C9): 2004JC002671. https://doi.org/10.1029/2004JC002671.

Callahan, Benjamin J, Paul J McMurdie, Michael J Rosen, Andrew W Han, Amy Jo A Johnson, e Susan P Holmes. 2016. «DADA2: High-Resolution Sample Inference from Illumina Amplicon Data». *Nature Methods* 13 (7): 581–83. https://doi.org/10.1038/nmeth.3869.

Carbonara, Pierluigi, e Maria Cristina Follesa, a c. di. 2019. *Handbook on Fish Age Determination: A Mediterranean Experience*. Rome: Food and Agriculture Organization of the United Nations.

Carden, A., R.M. Rajachar, M.D. Morris, e D.H. Kohn. 2003. «Ultrastructural Changes Accompanying the Mechanical Deformation of Bone Tissue: A Raman Imaging Study». *Calcified Tissue International* 72 (2): 166–75. https://doi.org/10.1007/s00223-002-1039-0.

Carden, Angela, e Michael D. Morris. 2000. «Application of Vibrational Spectroscopy to the Study of Mineralized Tissues (Review)». *Journal of Biomedical Optics* 5 (3): 259. https://doi.org/10.1117/1.429994.

Cattano, Carlo, Joachim Claudet, Paolo Domenici, e Marco Milazzo. 2018. «Living in a High CO_2 World: A Global Meta-analysis Shows Multiple Trait-mediated Fish Responses to Ocean Acidification». *Ecological Monographs* 88 (3): 320–35. https://doi.org/10.1002/ecm.1297.

Cattano, Carlo, Folco Giomi, e Marco Milazzo. 2016. «Effects of Ocean Acidification on Embryonic Respiration and Development of a Temperate Wrasse Living along a Natural CO_2 Gradient». *Conservation Physiology* 4 (1): cov073. https://doi.org/10.1093/conphys/cov073.

Checkley, David M., Andrew G. Dickson, Motomitsu Takahashi, J. Adam Radich, Nadine Eisenkolb, e Rebecca Asch. 2009. «Elevated CO_2 Enhances Otolith Growth in Young Fish». *Science* 324 (5935): 1683–1683. https://doi.org/10.1126/science.1169806.

Dando, P. R., J. A. Hughes, e F. Thiermann. 1995. «Preliminary Observations on Biological Communities at Shallow Hydrothermal Vents in the Aegean Sea». *Geological Society, London, Special Publications* 87 (1): 303–17. https://doi.org/10.1144/GSL.SP.1995.087.01.23.

Di Santo, Valentina. 2019. «Ocean Acidification and Warming Affect Skeletal Mineralization in a Marine Fish». *Proceedings of the Royal Society B: Biological Sciences* 286 (1894): 20182187. https://doi.org/10.1098/rspb.2018.2187.

Dixson, Danielle L., Philip L. Munday, e Geoffrey P. Jones. 2010. «Ocean Acidification Disrupts the Innate Ability of Fish to Detect Predator Olfactory Cues». *Ecology Letters* 13 (1): 68–75. https://doi.org/10.1111/j.1461-0248.2009.01400.x.

Do, H. H., P. Gronkjaer, e V. Simonsen. 2006. «Otolith Morphology, Microstructure and Ageing in the Hedgehog Seahorse, Hippocampus Spinosissimus (Weber, 1913)».

Journal of Applied Ichthyology 22 (2): 153–59. https://doi.org/10.1111/j.1439-0426.2006.00729.x.

Domenici, Paolo, Bridie Allan, Mark I. McCormick, e Philip L. Munday. 2012. «Elevated Carbon Dioxide Affects Behavioural Lateralization in a Coral Reef Fish». *Biology Letters* 8 (1): 78–81. https://doi.org/10.1098/rsbl.2011.0591.

Doney, Scott. 2009. «The Consequences of Human-Driven Ocean Acidification for Marine Life». *F1000 Biology Reports* 1 (maggio):36. https://doi.org/10.3410/B1-36.

Dziergwa, Jacqueline, Sarika Singh, Christopher R. Bridges, Sven E. Kerwath, Joachim Enax, e Lutz Auerswald. 2019. «Acid-Base Adjustments and First Evidence of Denticle Corrosion Caused by Ocean Acidification Conditions in a Demersal Shark Species». *Scientific Reports* 9 (1): 18668. https://doi.org/10.1038/s41598-019-54795-7.

Edgar, Robert C. 2013. «UPARSE: Highly Accurate OTU Sequences from Microbial Amplicon Reads». *Nature Methods* 10 (10): 996–98. https://doi.org/10.1038/nmeth.2604.

Edgar, Robert C., Brian J. Haas, Jose C. Clemente, Christopher Quince, e Rob Knight. 2011. «UCHIME Improves Sensitivity and Speed of Chimera Detection». *Bioinformatics* 27 (16): 2194–2200. https://doi.org/10.1093/bioinformatics/btr381.

EPICA community members. 2004. «Eight Glacial Cycles from an Antarctic Ice Core». *Nature* 429 (6992): 623–28. https://doi.org/10.1038/nature02599.

Farlay, Delphine, Gérard Panczer, Christian Rey, Pierre D. Delmas, e Georges Boivin. 2010. «Mineral Maturity and Crystallinity Index Are Distinct Characteristics of Bone Mineral». *Journal of Bone and Mineral Metabolism* 28 (4): 433–45. https://doi.org/10.1007/s00774-009-0146-7.

Feely, Richard A., Simone R. Alin, Jan Newton, Christopher L. Sabine, Mark Warner, Allan Devol, Christopher Krembs, e Carol Maloy. 2010. «The Combined Effects of Ocean Acidification, Mixing, and Respiration on pH and Carbonate Saturation in an Urbanized Estuary». *Estuarine, Coastal and Shelf Science* 88 (4): 442–49. https://doi.org/10.1016/j.ecss.2010.05.004.

Feely, Richard A, Scot T C Doney, e Sar Ah R Cooley. 2009. «Ocean Acidification».

Feely, Richard A., Christopher L. Sabine, Kitack Lee, Will Berelson, Joanie Kleypas, Victoria J. Fabry, e Frank J. Millero. 2004. «Impact of Anthropogenic CO_2 on the $CaCO_3$ System in the Oceans». *Science* 305 (5682): 362–66. https://doi.org/10.1126/science.1097329.

Fontes, Jorge, Pedro Afonso, Ricardo S. Santos, e Jennifer E. Caselle. 2010. «Temporal Variability of Larval Growth, Size, Stage Duration and Recruitment of a Wrasse, *Coris Julis* (Pisces: Labridae), from the Azores». *Scientia Marina* 74 (4): 721–29. https://doi.org/10.3989/scimar.2010.74n4721.

Foo, Shawna Andrea, Maria Byrne, e Maria Cristina Gambi. s.d. «THE CARBON DIOXIDE VENTS OF ISCHIA, ITALY, A NATURAL SYSTEM TO ASSESS IMPACTS OF OCEAN ACIDIFICATION ON MARINE ECOSYSTEMS: AN OVERVIEW OF RESEARCH AND COMPARISONS WITH OTHER VENT SYSTEMS».

Fratzl, P., H. S. Gupta, E. P. Paschalis, e P. Roschger. 2004. «Structure and Mechanical Quality of the Collagen–Mineral Nano-Composite in Bone». *J. Mater. Chem.* 14 (14): 2115–23. https://doi.org/10.1039/B402005G.

Gambi, Riccardo, Chiara Lombardi, Silvia Cocito, Jason M. Hall-Spencer, e Maria Cristina Gambi. 2010. «USING VOLCANIC MARINE CO2 VENTS TO STUDY THE EFFECTS OF OCEAN ACIDIFICATION ON BENTHIC BIOTA: HIGHLIGHTS FROM CASTELLO ARAGONESE D'ISCHIA (TYRRHENIAN SEA)». *Marine Ecology* 31 (3): 447–56. https://doi.org/10.1111/j.1439-0485.2009.00354.x.

Garcia-Rubies, A., e E. Macpherson. 1995. «Substrate Use and Temporal Pattern of Recruitment in Juvenile Fishes of the Mediterranean Littoral». *Marine Biology* 124 (1): 35–42. https://doi.org/10.1007/BF00349144.

Gattuso, J.-P., A. Magnan, R. Billé, W. W. L. Cheung, E. L. Howes, F. Joos, D. Allemand, et al. 2015. «Contrasting Futures for Ocean and Society from Different Anthropogenic CO 2 Emissions Scenarios». *Science* 349 (6243): aac4722. https://doi.org/10.1126/science.aac4722.

Glimcher, Melvin J. 1998. «The Nature of the Mineral Phase in Bone: Biological and Clinical Implications». In *Metabolic Bone Disease and Clinically Related Disorders*, 23–52e. Elsevier. https://doi.org/10.1016/B978-012068700-8/50003-7.

Gordoa, Ana, Balbina Molí, e Nuria Raventós. 2000. «Growth Performance of Four Wrasse Species on the North-Western Mediterranean Coast». *Fisheries Research* 45 (1): 43–50. https://doi.org/10.1016/S0165-7836(99)00094-6.

Goverts, Zoë, Paul Nührenberg, e Alex Jordan. 2021. «Environmental Reconstruction and Tracking as Methods to Explore Social Interactions in Marine Environments: A Test Case With the Mediterranean Rainbow Wrasse Coris Julis». *Frontiers in Marine Science* 8 (luglio):695100. https://doi.org/10.3389/fmars.2021.695100.

Guinotte, John M., e Victoria J. Fabry. 2008. «Ocean Acidification and Its Potential Effects on Marine Ecosystems». *Annals of the New York Academy of Sciences* 1134 (1): 320–42. https://doi.org/10.1196/annals.1439.013.

Hall-Spencer, Jason M., Riccardo Rodolfo-Metalpa, Sophie Martin, Emma Ransome, Maoz Fine, Suzanne M. Turner, Sonia J. Rowley, Dario Tedesco, e Maria-Cristina Buia. 2008. «Volcanic Carbon Dioxide Vents Show Ecosystem Effects of Ocean Acidification». *Nature* 454 (7200): 96–99. https://doi.org/10.1038/nature07051.

Heuer, Rachael M., e Martin Grosell. 2014. «Physiological Impacts of Elevated Carbon Dioxide and Ocean Acidification on Fish». *American Journal of Physiology-Regulatory, Integrative and Comparative Physiology* 307 (9): R1061–84. https://doi.org/10.1152/ajpregu.00064.2014.

Ina-Salwany, M. Y., Nurhidayu Al-saari, Aslah Mohamad, Fathin-Amirah Mursidi, Aslizah Mohd-Aris, M. N. A. Amal, Hisae Kasai, Sayaka Mino, Tomoo Sawabe, e M. Zamri-Saad. 2019. «Vibriosis in Fish: A Review on Disease Development and Prevention». *Journal of Aquatic Animal Health* 31 (1): 3–22. https://doi.org/10.1002/aah.10045.

Ishimatsu, Atsushi, Takashi Kikkawa, Masahiro Hayashi, Kyoung-Seon Lee, e Jun Kita. 2004. «Effects of CO2 on Marine Fish: Larvae and Adults». *Journal of Oceanography* 60 (4): 731–41. https://doi.org/10.1007/s10872-004-5765-y.

Jawad, Laith A. 2007. «Comparative Morphology of the Otolith of the Triplefins (Family: Tripterygiidae)». *Journal of Natural History* 41 (13–16): 901–24. https://doi.org/10.1080/00222930701342529.

Juraida, J, M Sontang, E A Ghapur, e M I N Isa. 2011. «PREPARATION AND CHARACTERIZATION OF HYDROXYAPATITE FROM FISHBONE».

Klindworth, Anna, Elmar Pruesse, Timmy Schweer, Jörg Peplies, Christian Quast, Matthias Horn, e Frank Oliver Glöckner. 2013. «Evaluation of General 16S Ribosomal RNA Gene PCR Primers for Classical and Next-Generation Sequencing-Based Diversity Studies». *Nucleic Acids Research* 41 (1): e1–e1. https://doi.org/10.1093/nar/gks808.

Koch, Marguerite, George Bowes, Cliff Ross, e Xing-Hai Zhang. 2013. «Climate Change and Ocean Acidification Effects on Seagrasses and Marine Macroalgae». *Global Change Biology* 19 (1): 103–32. https://doi.org/10.1111/j.1365-2486.2012.02791.x.

Kroeker, Kristy J., Rebecca L. Kordas, Ryan Crim, Iris E. Hendriks, Laura Ramajo, Gerald S. Singh, Carlos M. Duarte, e Jean-Pierre Gattuso. 2013. «Impacts of Ocean Acidification

on Marine Organisms: Quantifying Sensitivities and Interaction with Warming». *Global Change Biology* 19 (6): 1884–96. https://doi.org/10.1111/gcb.12179.

Kroeker, Kristy J., Rebecca L. Kordas, Ryan N. Crim, e Gerald G. Singh. 2010. «Meta-analysis Reveals Negative yet Variable Effects of Ocean Acidification on Marine Organisms». *Ecology Letters* 13 (11): 1419–34. https://doi.org/10.1111/j.1461-0248.2010.01518.x.

Kroeker, Kristy J., Fiorenza Micheli, Maria Cristina Gambi, e Todd R. Martz. 2011. «Divergent Ecosystem Responses within a Benthic Marine Community to Ocean Acidification». *Proceedings of the National Academy of Sciences* 108 (35): 14515–20. https://doi.org/10.1073/pnas.1107789108.

Kuziel, Gavin A., e Seth Rakoff-Nahoum. 2022. «The Gut Microbiome». *Current Biology* 32 (6): R257–64. https://doi.org/10.1016/j.cub.2022.02.023.

Labella, Alejandro M., M. Dolores Castro, Manuel Manchado, Teresa Lucena, David R. Arahal, e Juan J. Borrego. 2018. «Photobacterium Malacitanum Sp. Nov., and Photobacterium Andalusiense Sp. Nov., Two New Bacteria Isolated from Diseased Farmed Fish in Southern Spain». *Systematic and Applied Microbiology* 41 (5): 444–51. https://doi.org/10.1016/j.syapm.2018.04.005.

Labella, A.M., J.J. Rosado, M. Balado, M.L. Lemos, e J.J. Borrego. 2020. «Virulence Properties of Three New *Photobacterium* Species Affecting Cultured Fish». *Journal of Applied Microbiology* 129 (1): 37–50. https://doi.org/10.1111/jam.14437.

Laplante, Karine, Boutin Sébastien, e Nicolas Derome. 2013. «Parallel Changes of Taxonomic Interaction Networks in Lacustrine Bacterial Communities Induced by a Polymetallic Perturbation». *Evolutionary Applications* 6 (4): 643–59. https://doi.org/10.1111/eva.12050.

Lazado, Carlo C., e Christopher Marlowe A. Caipang. 2014. «Mucosal Immunity and Probiotics in Fish». *Fish & Shellfish Immunology* 39 (1): 78–89. https://doi.org/10.1016/j.fsi.2014.04.015.

Lescak, Emily A., e Kathryn C. Milligan-Myhre. 2017. «Teleosts as Model Organisms To Understand Host-Microbe Interactions». A cura di George O'Toole. *Journal of Bacteriology* 199 (15). https://doi.org/10.1128/JB.00868-16.

Leung, Jonathan Y. S., Ivan Nagelkerken, Jennifer C. A. Pistevos, Zonghan Xie, Sam Zhang, e Sean D. Connell. 2022. «Shark Teeth Can Resist Ocean Acidification». *Global Change Biology* 28 (7): 2286–95. https://doi.org/10.1111/gcb.16052.

March, D, M Palmer, J Alós, A Grau, e F Cardona. 2010. «Short-Term Residence, Home Range Size and Diel Patterns of the Painted Comber Serranus Scriba in a Temperate Marine Reserve». *Marine Ecology Progress Series* 400 (febbraio):195–206. https://doi.org/10.3354/meps08410.

Martin, Marcel. s.d. «&XWDGDSW_UHPRYHV_DGDSWHU_ VHTXHQFHV_IURP_KLJK_WKURXJKSXW_ VHTXHQFLQJ_UHDGV».

McCormick, Mark I., Sue-Ann Watson, e Philip L. Munday. 2013. «Ocean Acidification Reverses Competition for Space as Habitats Degrade». *Scientific Reports* 3 (1): 3280. https://doi.org/10.1038/srep03280.

Mecca, Silvia, Edoardo Casoli, Giandomenico Ardizzone, e Maria Cristina Gambi. 2020. «Effects of Ocean Acidification on Phenology and Epiphytes of the Seagrass Posidonia Oceanica at Two CO2 Vent Systems of Ischia (Italy)». *Mediterranean Marine Science* 21 (1): 70. https://doi.org/10.12681/mms.20795.

Melzner, F, M A Gutowska, M Langenbuch, S Dupont, M Lucassen, M C Thorndyke, e M Bleich. 2009. «Physiological Basis for High CO2 Tolerance in Marine Ectothermic Animals: Pre-Adaptation through Lifestyle and Ontogeny?»

Miller, Gabrielle M., Sue-Ann Watson, Mark I. McCormick, e Philip L. Munday. 2013. «Increased CO_2 Stimulates Reproduction in a Coral Reef Fish». *Global Change Biology* 19 (10): 3037–45. https://doi.org/10.1111/gcb.12259.

Miller, Lisa M, William Little, Anne Schirmer, Farhan Sheik, Bhavin Busa, e Stefan Judex. 2007. «Accretion of Bone Quantity and Quality in the Developing Mouse Skeleton». *Journal of Bone and Mineral Research* 22 (7): 1037–45. https://doi.org/10.1359/jbmr.070402.

Miller, Lisa M, Jaclyn Tetenbaum Novatt, David Hamerman, e Cathy S Carlson. 2004. «Alterations in Mineral Composition Observed in Osteoarthritic Joints of Cynomolgus Monkeys». *Bone* 35 (2): 498–506. https://doi.org/10.1016/j.bone.2004.03.034.

Miller, Lisa M., Vidyasagar Vairavamurthy, Mark R. Chance, Richard Mendelsohn, Eleftherios P. Paschalis, Foster Betts, e Adele L. Boskey. 2001. «In Situ Analysis of Mineral Content and Crystallinity in Bone Using Infrared Micro-Spectroscopy of the N4 PO43− Vibration». *Biochimica et Biophysica Acta (BBA) - General Subjects* 1527 (1–2): 11–19. https://doi.org/10.1016/S0304-4165(01)00093-9.

Mirasole, Alice, Bronwyn May Gillanders, Patrick Reis-Santos, Fausto Grassa, Giorgio Capasso, Giovanna Scopelliti, Antonio Mazzola, e Salvatrice Vizzini. 2017. «The Influence of High pCO2 on Otolith Shape, Chemical and Carbon Isotope Composition of Six Coastal Fish Species in a Mediterranean Shallow CO2 Vent». *Marine Biology* 164 (9): 191. https://doi.org/10.1007/s00227-017-3221-y.

Mirasole, Alice, Giovanna Scopelliti, Cecilia Tramati, Geraldina Signa, Antonio Mazzola, e Salvatrice Vizzini. 2021. «Evidences on Alterations in Skeleton Composition and Mineralization in a Site-Attached Fish under Naturally Acidified Conditions in a Shallow CO2 Vent». *Science of The Total Environment* 761 (marzo):143309. https://doi.org/10.1016/j.scitotenv.2020.143309.

Munday, P. L., V. Hernaman, D. L. Dixson, e S. R. Thorrold. 2011. «Effect of Ocean Acidification on Otolith Development in Larvae of a Tropical Marine Fish». *Biogeosciences* 8 (6): 1631–41. https://doi.org/10.5194/bg-8-1631-2011.

Munday, Philip L., Alistair J. Cheal, Danielle L. Dixson, Jodie L. Rummer, e Katharina E. Fabricius. 2014. «Behavioural Impairment in Reef Fishes Caused by Ocean Acidification at CO2 Seeps». *Nature Climate Change* 4 (6): 487–92. https://doi.org/10.1038/nclimate2195.

Munday, Philip L., Danielle L. Dixson, Jennifer M. Donelson, Geoffrey P. Jones, Morgan S. Pratchett, Galina V. Devitsina, e Kjell B. Døving. 2009. «Ocean Acidification Impairs Olfactory Discrimination and Homing Ability of a Marine Fish». *Proceedings of the National Academy of Sciences* 106 (6): 1848–52. https://doi.org/10.1073/pnas.0809996106.

Munday, Philip L, Geoffrey P Jones, Morgan S Pratchett, e Ashley J Williams. 2008. «Climate Change and the Future for Coral Reef Fishes». *Fish and Fisheries* 9 (3): 261–85. https://doi.org/10.1111/j.1467-2979.2008.00281.x.

Munday, Pl, M Gagliano, Jm Donelson, Dl Dixson, e Sr Thorrold. 2011. «Ocean Acidification Does Not Affect the Early Life History Development of a Tropical Marine Fish». *Marine Ecology Progress Series* 423 (febbraio):211–21. https://doi.org/10.3354/meps08990.

N., Raventós, e Macpherson E. 2001. «Planktonic Larval Duration and Settlement Marks on the Otoliths of Mediterranean Littoral Fishes». *Marine Biology* 138 (6): 1115–20. https://doi.org/10.1007/s002270000535.

Nagelkerken, Ivan, e Sean D. Connell. 2015. «Global Alteration of Ocean Ecosystem Functioning Due to Increasing Human CO_2 Emissions». *Proceedings of the National Academy of Sciences* 112 (43): 13272–77. https://doi.org/10.1073/pnas.1510856112.

Nayak, Sukanta K. 2010. «Role of Gastrointestinal Microbiota in Fish: Role of Gastrointestinal Microbiota in Fish». *Aquaculture Research* 41 (11): 1553–73. https://doi.org/10.1111/j.1365-2109.2010.02546.x.

Ng, Jenny C.Y., e Jill M.Y. Chiu. 2020. «Changes in Biofilm Bacterial Communities in Response to Combined Effects of Hypoxia, Ocean Acidification and Nutrients from Aquaculture Activity in Three Fathoms Cove». *Marine Pollution Bulletin* 156 (luglio):111256. https://doi.org/10.1016/j.marpolbul.2020.111256.

Nilsson, Göran E., Danielle L. Dixson, Paolo Domenici, Mark I. McCormick, Christina Sørensen, Sue-Ann Watson, e Philip L. Munday. 2012. «Near-Future Carbon Dioxide Levels Alter Fish Behaviour by Interfering with Neurotransmitter Function». *Nature Climate Change* 2 (3): 201–4. https://doi.org/10.1038/nclimate1352.

Orr, James C., Victoria J. Fabry, Olivier Aumont, Laurent Bopp, Scott C. Doney, Richard A. Feely, Anand Gnanadesikan, et al. 2005. «Anthropogenic Ocean Acidification over the Twenty-First Century and Its Impact on Calcifying Organisms». *Nature* 437 (7059): 681–86. https://doi.org/10.1038/nature04095.

Pan, Yuanming, e Michael E. Fleet. 2002. «2. Compositions of the Apatite-Group Minerals: Substitution Mechanisms and Controlling Factors». In *Phosphates*, a cura di Matthew J. Kohn, John Rakovan, e John M. Hughes, 13–50. De Gruyter. https://doi.org/10.1515/9781501509636-005.

Pankhurst, Ned W., e Philip L. Munday. 2011. «Effects of Climate Change on Fish Reproduction and Early Life History Stages». *Marine and Freshwater Research* 62 (9): 1015. https://doi.org/10.1071/MF10269.

Petit, J R, J Jouzel, D Raynaud, N I Barkov, G Delaygue, M Delmotte, V M Kotlyakov, et al. 1999. «Climate and Atmospheric History of the Past 420,000 Years from the Vostok Ice Core, Antarctica» 399.

Petit-Marty, Natalia, Ivan Nagelkerken, Sean D. Connell, e Celia Schunter. 2021a. «Natural CO_2 Seeps Reveal Adaptive Potential to Ocean Acidification in Fish». *Evolutionary Applications* 14 (7): 1794–1806. https://doi.org/10.1111/eva.13239.

———. 2021b. «Natural CO_2 Seeps Reveal Adaptive Potential to Ocean Acidification in Fish». *Evolutionary Applications* 14 (7): 1794–1806. https://doi.org/10.1111/eva.13239.

Piccoli, P. M., e P. A. Candela. 2002. «Apatite in Igneous Systems». *Reviews in Mineralogy and Geochemistry* 48 (1): 255–92. https://doi.org/10.2138/rmg.2002.48.6.

Pino, Claudio A, Luis A Cubillos, Miguel Araya, e Aquiles Sepúlveda. 2004. «Otolith Weight as an Estimator of Age in the Patagonian Grenadier, Macruronus Magellanicus, in Central-South Chile». *Fisheries Research*.

Ricevuto, Elena, K. J. Kroeker, F. Ferrigno, F. Micheli, e M. C. Gambi. 2014. «Spatio-Temporal Variability of Polychaete Colonization at Volcanic CO2 Vents Indicates High Tolerance to Ocean Acidification». *Marine Biology* 161 (12): 2909–19. https://doi.org/10.1007/s00227-014-2555-y.

Sabine, Christopher L., Richard A. Feely, Nicolas Gruber, Robert M. Key, Kitack Lee, John L. Bullister, Rik Wanninkhof, et al. 2004. «The Oceanic Sink for Anthropogenic CO_2». *Science* 305 (5682): 367–71. https://doi.org/10.1126/science.1097403.

Salinas, Irene. 2015. «The Mucosal Immune System of Teleost Fish». *Biology* 4 (3): 525–39. https://doi.org/10.3390/biology4030525.

Scopelliti, Giovanna, Rossella Di Leonardo, Cecilia D. Tramati, Antonio Mazzola, e Salvatrice Vizzini. 2015. «Premature Aging in Bone of Fish from a Highly Polluted Marine Area». *Marine Pollution Bulletin* 97 (1–2): 333–41. https://doi.org/10.1016/j.marpolbul.2015.05.069.

Shin, Na-Ri, Tae Woong Whon, e Jin-Woo Bae. 2015. «Proteobacteria: Microbial Signature of Dysbiosis in Gut Microbiota». *Trends in Biotechnology* 33 (9): 496–503. https://doi.org/10.1016/j.tibtech.2015.06.011.

Siegenthaler, Urs, Thomas F. Stocker, Eric Monnin, Dieter Lüthi, Jakob Schwander, Bernhard Stauffer, Dominique Raynaud, et al. 2005. «Stable Carbon CycleClimate Relationship During the Late Pleistocene». *Science* 310 (5752): 1313–17. https://doi.org/10.1126/science.1120130.

Signorini, Silvia Giorgia, Marco Munari, Antonio Cannavacciuolo, Matteo Nannini, Diletta Dolfini, Antonia Chiarore, Fiorenza Farè, et al. 2023. «Investigation of the Molecular Mechanisms Which Contribute to the Survival of the Polychaete Platynereis Spp. under Ocean Acidification Conditions in the CO2 Vent System of Ischia Island (Italy)». *Frontiers in Marine Science* 9 (gennaio):1067900. https://doi.org/10.3389/fmars.2022.1067900.

Simpson, Stephen D., Philip L. Munday, Matthew L. Wittenrich, Rachel Manassa, Danielle L. Dixson, Monica Gagliano, e Hong Y. Yan. 2011. «Ocean Acidification Erodes Crucial Auditory Behaviour in a Marine Fish». *Biology Letters* 7 (6): 917–20. https://doi.org/10.1098/rsbl.2011.0293.

Škeljo, Frane, Josipa Ferri, Jure Brčić, Mirela Petrić, e Ivan Jardas. 2012. «Age, Growth and Utility of Otolith Morphometrics as a Predictor of Age in the Wrasse *Coris Julis* (Labridae) from the Eastern Adriatic Sea». *Scientia Marina* 76 (3): 587–95. https://doi.org/10.3989/scimar.03521.07G.

Stransky, Christoph, Hannes Baumann, Svein-Erik Fevolden, Alf Harbitz, Hans Høie, Kjell H. Nedreaas, Arnt-Børre Salberg, e Tuula H. Skarstein. 2008. «Separation of Norwegian Coastal Cod and Northeast Arctic Cod by Outer Otolith Shape Analysis». *Fisheries Research* 90 (1–3): 26–35. https://doi.org/10.1016/j.fishres.2007.09.009.

Sylvain, François-Étienne, Bachar Cheaib, Martin Llewellyn, Tiago Gabriel Correia, Daniel Barros Fagundes, Adalberto Luis Val, e Nicolas Derome. 2016. «pH Drop Impacts Differentially Skin and Gut Microbiota of the Amazonian Fish Tambaqui (Colossoma Macropomum)». *Scientific Reports* 6 (1): 32032. https://doi.org/10.1038/srep32032.

Tarasov, V.G., A.V. Gebruk, A.N. Mironov, e L.I. Moskalev. 2005. «Deep-Sea and Shallow-Water Hydrothermal Vent Communities: Two Different Phenomena?» *Chemical Geology* 224 (1–3): 5–39. https://doi.org/10.1016/j.chemgeo.2005.07.021.

Tarkan, Ali Serhan, Çiğdem GÜRSOY Gaygusuz, Özcan Gaygusuz, e Hasan Acipinar. s.d. «Use of Bone and Otolith Measures for Size-Estimation of Fish in Predator-Prey Studies».

Tiralongo, Francesco, Giuseppina Messina, Bianca Maria Lombardo, Lucia Longhitano, Giovanni Li Volti, e Daniele Tibullo. 2020. «Skin Mucus of Marine Fish as a Source for the Development of Antimicrobial Agents». *Frontiers in Marine Science* 7 (settembre):541853. https://doi.org/10.3389/fmars.2020.541853.

Tuset, Víctor M., Paul L. Rosin, e Antonio Lombarte. 2006. «Sagittal Otolith Shape Used in the Identification of Fishes of the Genus Serranus». *Fisheries Research* 81 (2–3): 316–25. https://doi.org/10.1016/j.fishres.2006.06.020.

Volpedo, A. 2003. «Ecomorphological Patterns of the Sagitta in Fish on the Continental Shelf off Argentine». *Fisheries Research* 60 (2–3): 551–60. https://doi.org/10.1016/S0165-7836(02)00170-4.

Waessle, Juan A., Carlos A. Lasta, e Marco Favero. 2003. «Otolith Morphology and Body Size Relationships for Juvenile Sciaenidae in the Río de La Plata Estuary (35-36°S)». *Scientia Marina* 67 (2): 233–40. https://doi.org/10.3989/scimar.2003.67n2233.

White, James Robert, Niranjan Nagarajan, e Mihai Pop. 2009. «Statistical Methods for Detecting Differentially Abundant Features in Clinical Metagenomic Samples». A cura

di Christos A. Ouzounis. *PLoS Computational Biology* 5 (4): e1000352. https://doi.org/10.1371/journal.pcbi.1000352.

Wopenka, Brigitte, e Jill D. Pasteris. 2005. «A Mineralogical Perspective on the Apatite in Bone». *Materials Science and Engineering: C* 25 (2): 131–43. https://doi.org/10.1016/j.msec.2005.01.008.

Wynne, James W., Krishna K. Thakur, Joel Slinger, Francisca Samsing, Barry Milligan, James F. F. Powell, Allison McKinnon, et al. 2020. «Microbiome Profiling Reveals a Microbial Dysbiosis During a Natural Outbreak of Tenacibaculosis (Yellow Mouth) in Atlantic Salmon». *Frontiers in Microbiology* 11 (ottobre):586387. https://doi.org/10.3389/fmicb.2020.586387.